PHYSICAL REVIEW D VOLUME 12, NUMBER 9 1 NOVEMBER 1975

Application of current-algebra techniques to soft-pion production by the weak neutral current: V, A case *

Stephen L. Adler
The Institute for Advanced Study, Princeton, New Jersey 08540
(Received 21 April 1975)

We apply current-algebra techniques to study the constraints imposed on neutral-current-induced soft-pion production, using as input existing bounds on neutrino-proton elastic scattering and existing data on neutral-current-induced deep-inelastic scattering. In the case of a purely isoscalar weak neutral current, a simple soft-pion argument relates the cross section for threshold (in pion-nucleon invariant mass) weak pion production directly to the cross section for neutrino-proton elastic scattering. Hence, a bound on the latter cross section implies a bound on the former. To apply the method away from threshold and to nonisoscalar neutral currents, we extend a model which we had developed earlier for weak pion production in the (3,3) resonance region so as to include the low-energy-theorem constraints. Numerical work using the extended model shows that a threshold peak (now attributed to background) in preliminary Argonne data on $\nu + n \to \nu + p + \pi^-$ would have implied a threshold cross section much larger than can be obtained with any neutral current formed solely from members of the usual V, A nonets. We analyze recently reported Brookhaven National Laboratory results for neutral-current-induced soft-pion production under the simplifying assumption of a purely isoscalar V, A neutral current. We find in this case that the magnitude of the Brookhaven observations exceeds the theoretical maximum by more than a factor of 2 unless the assumed isoscalar current either contains a vector part with an anomalously large gyromagnetic ratio $|g| = |2M_N F_2/F_1|$ or involves the ninth (SU_3 singlet) axial-vector current. A vector part with a large $|g|$ value leads to characteristic modifications in the pion-nucleon invariant-mass spectrum for $M(\pi N) \leq 1.4$ GeV, an effect which should be testable in high-statistics experiments. Two other qualitative predictions of isoscalar V, A structures are (i) except for a narrow range of values of g, constructive V, A interference in $\nu + N \to \nu + N + \pi$ implies constructive interference in $\nu + p \to \nu + p$ and vice versa, and (ii) if V, A interference is observed in neutral weak processes then (as is well-known) the neutral interaction may make a parity-violating contribution to the pp, ep, and μp interactions. These features may help to distinguish V, A neutral-current couplings from alternative coupling types, which will be discussed in detail in subsequent papers of this series.

I. INTRODUCTION

The initial experiments discovering weak neutral currents in high-energy inclusive neutrino-nucleon scattering[1] have now been supplemented with the observation of neutral-current effects in the exclusive channel containing a pion-nucleon final state. Obtainable resolutions will permit the detailed study of pion-nucleon invariant-mass distributions in the region at and below the (3, 3) resonance. Some of the issues raised by recent Argonne National Laboratory (ANL)[2] and Brookhaven National Laboratory (BNL)[3] data on neutral-current exclusive channels are: (i) What is the expected magnitude for threshold (in invariant mass) neutral-current pion production? (ii) What are the implications if (3, 3) resonance excitation is not observed in neutral-current pion production? In the present paper we analyze these questions under the conventional assumption that the weak neutral current has a V, A spatial structure. A preliminary account of the analysis has appeared elsewhere.[4] In subsequent publications,[5] the same methods will be applied to the more general cases in which neutral-current couplings of S, P, T type appear, or in which V, A neutral currents with abnormal G parity are present.

The paper is organized as follows. In Sec. II we give a simple (although somewhat naive) analytic treatment of threshold pion production in the case when the neutral current is of pure isoscalar form, and use it to illustrate the methods employed in the more detailed treatments which follow. In Sec. III we develop the ingredients needed for a more elaborate treatment of bounds on soft-pion production. We first review the standard formulas describing neutrino-proton elastic scattering and deep-inelastic inclusive neutrino-nucleon scattering, the latter both in a general framework and within the context of quark-parton-model assumptions. We then describe the modifications needed to make our old dispersion-theoretic model for soft-pion production in the (3, 3) resonance region[6] consistent with all soft-pion theorem constraints, and discuss the inclusion of a well-defined set of corrections to the soft-pion limit. In Sec. IV we

give results of numerical studies of the pion production model, which show its validity in the charged current case. We then apply the formulas developed in Sec. III to a detailed numerical analysis of threshold pion production for the ANL neutrino flux case, considering a succession of more complex models for the structure of the neutral current, leading up to the most general neutral current which can be formed from members of the usual V,A nonets. We finally analyze low-invariant-mass $[W=M(\pi N)\leq 1.4\ \mathrm{GeV}]$ pion production for the BNL neutrino-flux spectrum, under the simplifying assumption of a pure isoscalar V,A neutral current. In Appendix A, we give the threshold low-energy theorem (analogous to that developed in Sec. II) which applies in the case of the $SU(2)\otimes U(1)$ model neutral current. In Appendix B, we attempt a rough estimate of the leading corrections to the soft-pion limit in the case of an isoscalar (octet) axial-vector current, and estimate the extent to which the corresponding corrections in the isovector current case are already included in the basic pion production model as a result of unitarization of the (3, 3) multipoles. In Appendix C, we discuss nuclear charge-exchange corrections for low-invariant-mass weak pion production and give a tabulation of the charge-exchange matrices for various nuclear targets of current theoretical interest.

II. SIMPLE ANALYTIC TREATMENT

We begin by giving a simple analytic treatment of threshold pion production, which, although somewhat naive, nonetheless illustrates the basic ideas exploited below in our more careful numerical calculations. The starting point for our derivation is the standard soft-pion formula[7] for pion emission in the process $\mathcal{J}+N\to\pi^j+N$, with $\mathcal{J}$ a general external current and N a nucleon. This reads[8]

$$\langle N(p_2)\,\pi(q)\,|\,\mathcal{J}(0)\,|\,N(p_1)\rangle = -\mathfrak{N}_{N\pi}\,\bar{u}(p_2)\Big[\frac{g_r}{M_N g_A}J_j'(k-q) - \frac{g_r}{2M_N}\not{q}\gamma_5\tau_j\frac{\not{p}_2+M_N}{M_\pi^2+2p_2\cdot q}J(k) - J(k)\frac{\not{p}_1+M_N}{M_\pi^2-2p_1\cdot q}\frac{g_r}{2M_N}\not{q}\gamma_5\tau_j + \text{possible additional pion-pole ``seagull'' contribution}\Big]u(p_1)\psi_j^* + O(q)\,, \tag{1}$$

with

$$\mathfrak{N}_N=\left(\frac{M_N}{p_{10}}\frac{M_N}{p_{20}}\right)^{1/2},\quad \mathfrak{N}_{N\pi}=\mathfrak{N}_N(2q_0)^{-1/2}\,,$$

$$\langle N(p_2)\,|\,\mathcal{J}(0)\,|\,N(p_1)\rangle \equiv \mathfrak{N}_N\,\bar{u}(p_2)J(p_2-p_1)u(p_1), \tag{2}$$

$$\langle N(p_2)\,|\,[F_j^5,\mathcal{J}(0)]\,|\,N(p_1)\rangle \equiv \mathfrak{N}_N\,\bar{u}(p_2)J_j'(p_2-p_1)u(p_1)\,.$$

In Eqs. (1) and (2), $k=p_2+q-p_1$ denotes the four-momentum carried by the external current, $g_r\approx 13.5$ is the pion-nucleon coupling constant, $g_A\approx 1.24$ is the nucleon axial-vector renormalization constant, $\bar{u}(p_2)$, $u(p_1)$ are nucleon spinors (including isospinors), and ψ_j is the isospin wave function of the emitted pion. The first term on the right-hand side of Eq. (1) is the usual equal-time commutator term which appears in soft-pion theorems, while the second and third terms are external-line-insertion terms in which the soft pion is emitted, respectively, from the final and initial nucleon lines. The additional pion-pole "seagull" piece[9] is necessary only when the pion-pole contributions of the first three terms do not add up to give the full pion-pole contribution expected for the reaction $\mathcal{J}+N\to\pi^j+N$.

Let us now specialize to the case of an isoscalar V,A external current $\mathcal{J}$, for which the equal-time commutator term vanishes[10] and for which there is no additional pion-pole "seagull" contribution. The entire soft-pion emission amplitude then comes from the external-line-insertion terms, which are most conveniently evaluated in the isobaric frame in which the final pion-nucleon system is at rest. In this frame, the insertion on the outgoing nucleon line vanishes at threshold in invariant mass, since when $\vec{p}_2=\vec{q}=0$ we have

$$\bar{u}(p_2)\not{q}\gamma_5(\not{p}_2+M_N)\big|_{\vec{p}_2=\vec{q}=0} = q_0\,\bar{u}(p_2)\gamma_0\gamma_5(\not{p}_2+M_N)\big|_{\vec{p}_2=0} = 0\,. \tag{3}$$

So at threshold, for an isoscalar V,A current $\mathcal{J}$, the matrix element of Eq. (1) reduces to the single term

$$\langle N(p_2)\,\pi(q)\,|\,\mathcal{J}(0)\,|\,N(p_1)\rangle = \mathfrak{N}_{N\pi}\,\bar{u}(p_2)J(k)\frac{\not{p}_1+M_N}{M_\pi-2p_{10}}\frac{g_r}{2M_N}\gamma_0\gamma_5\tau_j u(p_1)\psi_j^*\,. \tag{4}$$

On replacing the projection operator $(\not{p}_1+M_N)/2M_N$

by $\sum_s u(p_1 s)\,\bar{u}(p_1 s)$ and explicitly indicating the nucleon isospinors $\chi_2^\dagger, \chi_1$ and the helicity s_1 of the initial nucleon spinor $u(p_1)$, we find

$$\langle N(p_2)\,\pi(q)\,|\,\mathcal{J}(0)\,|\,N(p_1)\rangle = \sum \mathfrak{M}_{N\pi}\,\bar{u}(p_2)\,J(k)\,u(p_1 s)\,\frac{g_r}{M_\pi - 2p_{10}} \times[\bar{u}(p_1 s)\,\gamma_0\gamma_5\,u(p_1 s_1)]\,a\,, \tag{5}$$

with

$$a = \chi_2^\dagger\,\tau_j\,\chi_1\psi_j^* = \begin{cases} 1 \text{ for } p\to p+\pi^0 \\ -1 \text{ for } n\to n+\pi^0 \\ \sqrt{2} \text{ for } n\to p+\pi^- \\ \sqrt{2} \text{ for } p\to n+\pi^+ \end{cases} \tag{6}$$

The factor in square brackets in Eq. (5) is readily evaluated by using explicit expressions for the spinors, giving

$$\begin{aligned}\bar{u}(p_1 s)\,\gamma_0\gamma_5\,u(p_1 s_1) &= \left(\frac{p_{10}+M_N}{2M_N}\right)\chi_s^\dagger\left(1,\ \frac{\vec{\sigma}\cdot\vec{k}}{p_{10}+M_N}\right) \times\begin{pmatrix} 0 & 1 \\ -1 & 0\end{pmatrix}\begin{pmatrix} 1 \\ -\vec{\sigma}\cdot\vec{k}/(p_{10}+M_N)\end{pmatrix}\chi_{s_1} \\ &= -\chi_s^\dagger\,\frac{\vec{\sigma}\cdot\vec{k}}{M_N}\,\chi_{s_1} \\ &= \frac{|\vec{k}|}{M_N}\,\delta_{ss_1}s_1\,,\end{aligned} \tag{7}$$

where we have used the definition

$$-\vec{\sigma}\cdot\hat{k}\,\chi_{s_1} = s_1\chi_{s_1} \tag{8}$$

of the initial-state helicity. Since $s_1 = \pm 1$, this factor disappears when we square and sum over initial and final nucleon spins, so we get

$$\begin{aligned}\tfrac{1}{2}\sum_{N\text{ spins}} |\langle N(p_2)\,\pi(q)\,|\,\mathcal{J}(0)\,|\,N(p_1)\rangle|^2 &\equiv \mathfrak{N}_{N\pi}{}^2\langle|\mathfrak{M}_\pi|^2\rangle_{\text{threshold}} \\ &= \mathfrak{N}_{N\pi}{}^2\left[\tfrac{1}{2}\sum_N\sum_{\text{spins}}|\bar{u}(p_2)\,J(k)\,u(p_1)|^2\right] \times\left(\frac{g_r}{M_\pi - 2p_{10}}\right)^2\frac{|\vec{k}|^2}{M_N{}^2}\,a^2\,.\end{aligned} \tag{9}$$

If we now make the approximation of neglecting the pion mass in all kinematics, the factor in square brackets in Eq. (9) becomes just the squared, spin-averaged matrix element $\langle|\mathfrak{M}|^2\rangle$ for νN elastic scattering, and Eq. (9) tells us that

$$\begin{aligned}\langle|\mathfrak{M}_\pi|^2\rangle_{\text{threshold}} &= \langle|\mathfrak{M}|^2\rangle\left(\frac{g_r}{2M_N}\right)^2 a^2\,\frac{|\vec{k}|^2}{p_{10}{}^2} \\ &= \langle|\mathfrak{M}|^2\rangle\left(\frac{g_r}{2M_N}\right)^2 a^2\,\frac{t}{M_N{}^2}\,\frac{(1+t/4M_N{}^2)}{(1+t/2M_N{}^2)^2}\,,\quad t=-k^2\,.\end{aligned} \tag{10}$$

Inserting phase-space factors according to

$$\begin{aligned}\frac{d\sigma(\nu+p\to\nu+p)}{dt} &= \frac{1}{4\pi}\,\frac{1}{E^2}\,m_\nu{}^2\langle|\mathfrak{M}|^2\rangle\,, \\ \frac{d\sigma(\nu+N\to\nu+N+\pi)}{dt\,dW} &= \frac{1}{16\pi^3}\,\frac{|\vec{q}|}{E^2}\,m_\nu{}^2\langle|\mathfrak{M}_\pi|^2\rangle\,,\end{aligned} \tag{11}$$

with $|\vec{q}|$ the pion isobaric frame three-momentum, W the invariant mass of the final πN isobar, and E the initial lab neutrino energy, we get finally the relation

$$\frac{1}{|\vec{q}|}\,\frac{d\sigma(\nu+N\to\nu+N+\pi)}{dt\,dW}\bigg|_{\text{threshold}} = \frac{a^2}{4\pi^2 M_\pi{}^2}\left(\frac{g_r M_\pi}{2M_N}\right)^2\frac{t}{M_N{}^2}\left(1+\frac{t}{4M_N{}^2}\right)\times\left(1+\frac{t}{2M_N{}^2}\right)^{-2}\frac{d\sigma(\nu+p\to\nu+p)}{dt}\,, \tag{12}$$

$$a^2 = \begin{cases} 1 \text{ for } \pi^0 \text{ production} \\ 2 \text{ for } \pi^\pm \text{ production}\,. \end{cases}$$

We see that in the special case which has been under consideration, instead of obtaining a soft-pion relation between matrix elements, we obtain a relation directly in terms of reaction cross sections. *The significance of Eq. (12) is that it allows one to translate an upper bound on the strength of $\nu+p\to\nu+p$ into an upper bound on the strength of threshold pion production by the weak neutral current.*

As an illustration, let us apply Eq. (12) to the ANL data[2] by integrating over t and averaging over the ANL neutrino energy flux[11] $n_{\text{ANL}}(E)$, giving

$$\int dE\,n_{\text{ANL}}(E)\,\frac{M_N{}^2}{|\vec{q}|}\,\frac{d\sigma(\nu+n\to\nu+p+\pi^-)}{dW} = \frac{2}{4\pi^2}\,\frac{M_N{}^2}{M_\pi{}^2}\left(\frac{g_r M_\pi}{2M_N}\right)^2\int dE\,n_{\text{ANL}}(E)\int_0^{t_{\max}(E)} dt\,\frac{t}{M_N{}^2}\left(1+\frac{t}{4M_N{}^2}\right)\left(1+\frac{t}{2M_N{}^2}\right)^{-2}\frac{d\sigma(\nu+p\to\nu+p)}{dt}\,. \tag{13}$$

We have multiplied both sides of Eq. (12) by M_N^2 so that they have the dimensions of a cross section; also for convenience, we assume the flux $n_{\rm ANL}(E)$ to be unit normalized,

$$\int dE\, n_{\rm ANL}(E) = 1 \,, \tag{14}$$

so that we are considering flux-averaged cross sections. Using the ANL 95% confidence bound[12]

$$\sigma^{\rm ANL}(\nu + p \to \nu + p) \leq 0.32\, \sigma^{\rm ANL}(\nu + n \to \mu^- + p) \approx 0.25 \times 10^{-38}\ {\rm cm}^2 \,, \tag{15}$$

and assuming the t dependence of the charged-current quasielastic and neutral-current elastic cross sections to be similar,[13,14] we find that the right-hand side of Eq. (13) is bounded by $0.32 \times 0.46 \times 10^{-38}\ {\rm cm}^2 = 0.15 \times 10^{-38}\ {\rm cm}^2$. Using 20-MeV invariant-mass bins, we can then estimate a bound on the flux-averaged cross section in the two bins nearest threshold as shown in Table I, giving the result

$$\sigma^{\rm ANL}_{\rm 2\,bin} \equiv \sigma(\nu + n \to \nu + p + \pi^-\ {\rm ANL\ flux\ averaged},\ 1.08\ {\rm GeV} \leq W \leq 1.12\ {\rm GeV}) \leq 0.6 \times 10^{-41}\ {\rm cm}^2 \,. \tag{16}$$

For comparison, the preliminary ANL data on $\nu + n \to \nu + p + \pi^-$, before final background subtraction, showed ~5 events in the first two bins, which would have corresponded to a cross section of

$$\sigma^{\rm ANL}_{\rm 2\,bin}\ ({\rm before\ background\ subtraction}) \sim 20 \times 10^{-41}\ {\rm cm}^2 \,, \tag{17}$$

in strong violation of the bound of Eq. (16). It is now considered very probable that these events do *not* represent a true neutral-current effect, but arise from various neutron-induced backgrounds.

As we have already remarked, the above treatment is too naive in a number of respects. First of all, the restriction to cases, such as[10] that of an isoscalar neutral current $\mathcal{J}$, for which the equal-time commutator term vanishes excludes from consideration such processes as π^- production in the SU(2) ⊗ U(1) gauge model. Secondly, the external-line-insertion terms are rapidly varying pole terms, and so the kinematic approximation of neglecting M_π in calculating them can be dangerous. Finally, it is important to estimate the leading $O(q)$ corrections to the soft-pion approximation, and to calculate the effects in the threshold region of the tail of the (3, 3) resonance. As discussed in detail in Sec. III, we deal with these problems by using an extended version of a model for the weak pion-production amplitude which we have described elsewhere.[6] The extension will permit us to study the entire low-invariant-mass region $W \leq 1.4$ GeV, rather than just the first 40 MeV or so around threshold. For completeness, however, we give in Appendix A the analog of the threshold low-energy theorem of Eq. (12) for the case of the SU(2) ⊗ U(1)-model neutral current. The formulas of Appendix A still neglect the pion mass in the kinematics [as well as the leading $O(q)$ corrections and the (3, 3) resonance tail] and are not used in the subsequent numerical work.

III. DETAILED TREATMENT

We proceed in this section to set out the basis for a more detailed numerical treatment of bounds on weak pion production by a V, A weak neutral current. The basic idea, as developed above, is to use soft-pion techniques to relate weak pion production to elastic neutrino-proton scattering, and to use experimental bounds on the latter. It will also be useful, at some stages of the analysis, to impose constraints obtained from experimental data[1,15] on deep-inelastic inclusive neutrino-nucleon scattering induced by the weak neutral current. In Sec. III A we give the necessary vertex structure and cross-section formulas needed to describe neutrino-nucleon elastic scattering. In Sec. III B we give the necessary formulas for using deep-inelastic information; first, in a rather general form assuming only scaling and the fact that

$$\sigma(\bar\nu + N \to \mu^+ + \Gamma)/\sigma(\nu + N \to \mu^- + \Gamma) \approx \tfrac{1}{3} \,,$$

TABLE I. Application of Eq. (13) to bound the cross section for $\nu + n \to \nu + p + \pi^-$ in the two ANL 20-MeV bins nearest invariant-mass threshold.

W at bin center	$\lvert\vec{q}\rvert/M_N$	dW/M_N	Bound on right-hand side of Eq. (13)	Bound on cross section in bin $[(\lvert\vec{q}\rvert dW/M_N^2) \times 0.15 \times 10^{-38}\ {\rm cm}^2]$
1.09	6.4×10^{-2}	0.021	$0.15 \times 10^{-38}\ {\rm cm}^2$	$0.20 \times 10^{-41}\ {\rm cm}^2$
1.11	1.1×10^{-1}	0.021	$0.15 \times 10^{-38}\ {\rm cm}^2$	$0.35 \times 10^{-41}\ {\rm cm}^2$

and then in a more restrictive form which makes use of quark-parton model and quark-model assumptions. Finally, in Sec. III C we develop the extended weak-pion-production model which remedies the defects in our naive treatment enumerated at the end of Sec. II.

A. Elastic neutrino-nucleon scattering

We shall consider in what follows the most general V,A weak neutral current which can be formed from members of the usual vector and axial-vector nonets. We write for the neutral-current effective Lagrangian

$$\mathcal{L}_{\rm eff}^{N} = \frac{G}{\sqrt{2}}\,\bar{\nu}\gamma_\lambda(1-\gamma_5)\,\nu\mathcal{J}_N^\lambda ,$$
$$\mathcal{J}_N^\lambda = g_{V0}\mathcal{F}_0^\lambda + g_{V3}\mathcal{F}_3^\lambda + g_{V8}\mathcal{F}_8^\lambda - g_{A0}\mathcal{F}_0^{5\lambda} - g_{A3}\mathcal{F}_3^{5\lambda} - g_{A8}\mathcal{F}_8^{5\lambda} , \tag{18}$$

with $\mathcal{F}_j^\lambda$, $\mathcal{F}_j^{5\lambda}$ nonet currents represented in the quark model (with quark field ψ) by[16]

$$\mathcal{F}_j^\lambda = \bar{\psi}\gamma^\lambda\tfrac{1}{2}\lambda_j\psi ,$$
$$\mathcal{F}_j^{5\lambda} = \bar{\psi}\gamma^\lambda\gamma_5\tfrac{1}{2}\lambda_j\psi . \tag{19}$$

We express the nucleon matrix elements of the neutral members of these current nonets in the form[16]

$$\langle N(p_2)|\,\mathcal{F}_j^\lambda\,|N(p_1)\rangle = \mathcal{N}_N\bar{u}(p_2)[F_1^{(j)}(k^2)\gamma^\lambda + iF_2^{(j)}(k^2)\sigma^{\lambda\eta}k_\eta]t_j u(p_1) ,$$
$$\langle N(p_2)|\,\mathcal{F}_j^{5\lambda}\,|N(p_1)\rangle = \mathcal{N}_N\bar{u}(p_2)[g_A^{(j)}(k^2)\gamma^\lambda\gamma_5 + h_A^{(j)}(k^2)k^\lambda\gamma_5]t_j u(p_1) , \tag{20}$$
$$t_0 = \tfrac{1}{2}(\tfrac{2}{3})^{1/2},\quad t_3 = \tfrac{1}{2}\tau_3,\quad t_8 = \tfrac{1}{2}(\tfrac{1}{3})^{1/2} .$$

The vector and axial-vector form factors defined in Eq. (20) are related to the standard nucleon form factors $F_{1,2}^{V,S}(k^2)$, $g_A(k^2)$, $h_A(k^2)$ by

$$F_{1,2}^{(3)}(k^2) = F_{1,2}^{V}(k^2),\quad g_A^{(3)}(k^2) = g_A(k^2) ,$$
$$F_{1,2}^{(8)}(k^2) = 3F_{1,2}^{S}(k^2),\quad h_A^{(3)}(k^2) = h_A(k^2) . \tag{21}$$

Defining total form factors $F_{1,2}^{T}(k^2)$, $g_A^T(k^2)$ by

$$F_{1,2}^{T}(k^2) = \tfrac{1}{2}(\tfrac{2}{3})^{1/2}g_{V0}F_{1,2}^{(0)}(k^2) + \tfrac{1}{2}\epsilon\, g_{V3}F_{1,2}^{(3)}(k^2) + \tfrac{1}{2}(\tfrac{1}{3})^{1/2}g_{V8}F_{1,2}^{(8)}(k^2) ,$$
$$g_A^{T}(k^2) = \tfrac{1}{2}(\tfrac{2}{3})^{1/2}g_{A0}g_A^{(0)}(k^2) + \tfrac{1}{2}\epsilon\, g_{A3}g_A^{(3)}(k^2) + \tfrac{1}{2}(\tfrac{1}{3})^{1/2}g_{A8}g_A^{(8)}(k^2) , \tag{22}$$

with $\epsilon = 1$ for $\nu+p\to\nu+p$ and $\epsilon = -1$ for $\nu+n\to\nu+n$, the differential cross section for neutrino-nucleon scattering takes the form

$$\frac{d\sigma(\nu+N\to\nu+N)}{dt} = \frac{G^2}{8\pi E^2 M_N{}^2}\{[|F_1^T|^2 + |g_A^T|^2 + t|F_2^T|^2][4M_N{}^2E^2 - t(M_N{}^2+2M_NE)]$$
$$+\tfrac{1}{2}t[|g_A^T|^2(t+4M_N{}^2) + |F_1^T+2M_NF_2^T|^2 t] + \mathrm{Re}[g_A^{T*}(F_1^T+2M_NF_2^T)]t(4M_NE-t)\} . \tag{23}$$

For incident antineutrinos, the sign of g_A^T in Eq. (23) is reversed.

B. Deep-inelastic inclusive neutrino-nucleon scattering

We turn next to the constraints on the coefficients appearing in Eq. (18) which are imposed by experimental measurements[1,15] of the deep-inelastic inclusive neutrino-nucleon scattering ratios[8]

$$R_\nu \equiv \sigma(\nu+N\to\nu+\Gamma)/\sigma(\nu+N\to\mu^-+\Gamma) ,$$
$$R_{\bar\nu} \equiv \sigma(\bar\nu+N\to\bar\nu+\Gamma)/\sigma(\bar\nu+N\to\mu^++\Gamma) . \tag{24}$$

The charged-current-induced reactions in the denominators in Eq. (24) are described by the usual charged-current effective Lagrangian

$$\mathcal{L}_{\rm eff}^{\rm ch} = \frac{G}{\sqrt{2}}\,\bar{\mu}\gamma_\lambda(1-\gamma_5)\,\nu\mathcal{J}_{\rm ch}^\lambda + \text{adjoint} , \tag{25}$$

with

$$\mathcal{J}_{\rm ch}^\lambda = \cos\theta_C(\mathcal{F}_{1+i2}^\lambda - \mathcal{F}_{1+i2}^{5\lambda}) + \sin\theta_C(\mathcal{F}_{4+i5}^\lambda - \mathcal{F}_{4+i5}^{5\lambda}) . \tag{26a}$$

In what follows we aim only at getting formulas which hold to an accuracy of 10 or 20%, and so we make at the outset the approximation of taking the Cabibbo angle θ_C to be zero, which simplifies Eq. (26a) to read

$$\mathcal{J}_{\rm ch}^\lambda \approx \mathcal{F}_{1+i2}^\lambda - \mathcal{F}_{1+i2}^{5\lambda} . \tag{26b}$$

The virtue of using Eq. (26b) is that the vector and axial-vector parts of the charged current are then related by an isospin rotation to the corre-

sponding isovector vector and axial-vector terms in the neutral current of Eq. (18).

To proceed with the analysis, we assume the validity of Bjorken scaling[17] in deep-inelastic charged-current and neutral-current-induced inclusive neutrino reactions. Considering for the moment the charged-current cross sections $\sigma(\nu+N\to\mu^-+\Gamma)$ and $\sigma(\bar{\nu}+N\to\mu^++\Gamma)$, we review a standard analysis[18] starting from the formula

$$\frac{\sigma(\bar{\nu}+N\to\mu^++\Gamma)}{\sigma(\nu+N\to\mu^-+\Gamma)} = \frac{\int_0^1 dx\, a_S+\frac{1}{3}\int_0^1 dx\, x a_L+\int_0^1 dx\, x a_R}{\int_0^1 dx\, a_S+\int_0^1 dx\, x a_L+\frac{1}{3}\int_0^1 dx\, x a_R}, \quad (27)$$

where

$$a_S=\tfrac{1}{2}F_2-xF_1\geq 0\ ,$$
$$a_L=F_1-\tfrac{1}{2}F_3\geq 0\ ,$$
$$a_R=F_1+\tfrac{1}{2}F_3\geq 0\ ,$$
$$x=1/\omega=\text{scaling variable}\ ,$$

with $F_{1,2,3}$ the deep-inelastic structure functions in the scaling limit, and where an average nucleon target $N=\frac{1}{2}(n+p)$ has been assumed. Empirically, it is found that

$$\sigma(\bar{\nu}+N\to\mu^++\Gamma)/\sigma(\nu+N\to\mu^-+\Gamma)\approx\tfrac{1}{3}\ ,$$

which implies that $a_S\approx a_R\approx 0$, that is,

$$F_3(x)\approx -2F_1(x),\quad F_2(x)\approx 2xF_1(x)\ . \quad (28)$$

Splitting F_1 and F_2 into vector and axial-vector contributions

$$F_{1,2}(x)=F^V_{1,2}(x)+F^A_{1,2}(x)\ , \quad (29)$$

we may rewrite the relations of Eq. (28) as

$$\begin{aligned}&\tfrac{1}{4}|F_3(x)|\approx\tfrac{1}{2}[F^V_1(x)+F^A_1(x)]\ ,\\ &F^V_2(x)+F^A_2(x)\approx 2x[F^V_1(x)+F^A_1(x)]\ .\end{aligned} \quad (30)$$

Comparing Eq. (30) with the Schwarz inequality[19]

$$\tfrac{1}{4}|F_3(x)|\leq[F^V_1(x)\,F^A_1(x)]^{1/2}\leq\tfrac{1}{2}[F^V_1(x)+F^A_1(x)] \quad (31)$$

and the positivity inequalities

$$\begin{aligned}&F^V_2(x)\geq 2xF^V_1(x)\ ,\\ &F^A_2(x)\geq 2xF^A_1(x)\ ,\end{aligned} \quad (32)$$

we learn that

$$F^V_1(x)\approx F^A_1(x)\approx\frac{1}{2x}F^V_2(x)\approx\frac{1}{2x}F^A_2(x)$$
$$\approx-\tfrac{1}{4}F_3(x)\approx\tfrac{1}{2}F_1(x)\approx\frac{1}{4x}F_2(x)\ . \quad (33)$$

Now let us turn our attention to the deep-inelastic ratios of Eq. (24). If we again take N to be an average nucleon target, the isovector and isoscalar terms in the neutral current of Eq. (18) do not interfere, and so we get a lower bound on R_ν and $R_{\bar{\nu}}$ by neglecting the isoscalar contributions to the cross section. Using the fact, already mentioned, that the isovector pieces of Eq. (18) are related to the corresponding isovector pieces of Eq. (26) by an isospin rotation, we find that

$$\binom{R_\nu}{R_{\bar{\nu}}}\geq\frac{1}{2}\,\frac{\int_0^1 dx\{g_{V3}{}^2[\frac{1}{3}xF^V_1(x)+\frac{1}{2}F^V_2(x)]+g_{A3}{}^2[\frac{1}{3}xF^A_1(x)+\frac{1}{2}F^A_2(x)]\mp g_{V3}g_{A3}\frac{1}{3}xF_3(x)\}}{\int_0^1 dx[\frac{1}{3}xF_1(x)+\frac{1}{2}F_2(x)\mp\frac{1}{3}xF_3(x)]}\ . \quad (34)$$

Substituting now the relations of Eq. (33), we get the simple inequalities[20]

$$\begin{aligned}&R_\nu\geq\tfrac{1}{6}(g_{V3}{}^2+g_{A3}{}^2+g_{V3}g_{A3})\ ,\\ &R_{\bar{\nu}}\geq\tfrac{1}{2}(g_{V3}{}^2+g_{A3}{}^2-g_{V3}g_{A3})\ .\end{aligned} \quad (35)$$

When added in the linear combination $3R_\nu+R_{\bar{\nu}}$ which eliminates the vector–axial-vector interference term, and combined with 95% confidence limits inferred from current measurements of R_ν and $R_{\bar{\nu}}$, the inequalities of Eq. (35) yield the constraint

$$1.5\geq 3R_\nu+R_{\bar{\nu}}\geq g_{V3}{}^2+g_{A3}{}^2\ , \quad (36)$$

which will be used in our subsequent analysis. As we have already emphasized, in getting Eq. (36) we have only used the assumption of scaling together with the empirical observation of a charged-current antineutrino-to-neutrino inclusive cross-section ratio of $\approx\frac{1}{3}$.

In order to strengthen Eq. (36) so as to include the isoscalar current terms in Eq. (18), it is necessary to go beyond the assumptions just stated by using information from the quark-parton model. Specifically, we will make use of the standard spin-$\frac{1}{2}$ quark-parton model for deep-inelastic scattering,[21] with the additional assumptions that the strange parton and the antiparton content of the nucleon may be neglected[22] [the latter of these assumptions is suggested by the approximate relations of Eq. (33)]. The quark-parton model in this form is expected[22] to be good to an accuracy of order 20%, and has the great virtue that all x dependence (for an average nucleon target) appears in a single universal over-all factor which drops out in the ratios $R_{\nu,\bar{\nu}}$. A straightforward calculation then gives

$$\begin{pmatrix} R_\nu \\ \tfrac{1}{3}R_{\bar\nu} \end{pmatrix} = \tfrac{2}{3}\{[g_{V0}\tfrac{1}{2}(\tfrac{2}{3})^{1/2}+g_{V8}\tfrac{1}{2}(\tfrac{1}{3})^{1/2}]^2+(\tfrac{1}{2}g_{V3})^2+[g_{A0}\tfrac{1}{2}(\tfrac{2}{3})^{1/2}+g_{A8}\tfrac{1}{2}(\tfrac{1}{3})^{1/2}]^2+(\tfrac{1}{2}g_{A3})^2\}$$
$$\pm\tfrac{2}{3}\{[g_{V0}\tfrac{1}{2}(\tfrac{2}{3})^{1/2}+g_{V8}\tfrac{1}{2}(\tfrac{1}{3})^{1/2}][g_{A0}\tfrac{1}{2}(\tfrac{2}{3})^{1/2}+g_{A8}\tfrac{1}{2}(\tfrac{1}{3})^{1/2}]+\tfrac{1}{2}g_{V3}\tfrac{1}{2}g_{A3}\}\ , \tag{37}$$
$$1.5 \geq R_{\bar\nu}+3R_\nu = [g_{V0}(\tfrac{2}{3})^{1/2}+g_{V8}(\tfrac{1}{3})^{1/2}]^2+g_{V3}{}^2+[g_{A0}(\tfrac{2}{3})^{1/2}+g_{A8}(\tfrac{1}{3})^{1/2}]^2+g_{A3}{}^2\ .$$

One additional piece of information which will be needed, in order to use the constraint of Eq. (37) in an analysis of low-energy pion production, is knowledge of the renormalization constants $g_A^{(0,8)}(0)$ and $F_2^{(0,8)}(0)$ which describe the one-nucleon matrix elements of the isoscalar currents appearing in Eq. (18). The constant $g_A^{(8)}(0)$ is fairly reliably fixed by SU(3) to have the value[23]

$$g_A^{(8)}(0) \approx (3-4\times 0.66)\,1.24 = 0.45\ , \tag{38a}$$

while the measured value of $F_2^{(8)}(0)$ is

$$2M_N F_2^{(8)}(0)/F_1^{(8)}(0) = -0.12\ . \tag{38b}$$

For the constants $g_A^{(0)}(0)$ and $F_2^{(0)}(0)$ recourse must be made to a quark-model analysis of current-renormalization constants,[16] which gives[24]

$$g_A^{(0)}(0) \approx \tfrac{3}{5}\,1.24 = 0.74\ ,$$
$$2M_N F_2^{(0)}(0)/F_1^{(0)}(0) \approx -0.1 \tag{39}$$

for the unitary-singlet renormalization constants.

C. Extended model for weak pion production

We turn finally to a description of the extended model for weak pion production which we will use in the numerical calculations of Sec. IV. As an aid to the discussion which follows, let us first rewrite the pion-production matrix element of Eq. (1) in an alternative form, obtained by rearranging the pseudovector-coupling external-nucleon-line-insertion terms which appear there into pseudoscalar-coupling Born terms of the usual form. This gives

$$\langle N(p_2)\,\pi(q)\,|\mathcal{J}(0)|\,N(p_1)\rangle = -\mathfrak{N}_{N\pi}\,\bar u(p_2)\Big[\frac{g_r}{M_N g_A}J_j'(k-q)+\frac{g_r}{2M_N}\{\gamma_5\tau_j, J(k)\}_+$$
$$+\frac{g_r}{2M_N}\gamma_5\tau_j\frac{\not p_2+\not q+M_N}{\nu-\nu_B}J(k)-J(k)\frac{\not p_1-\not q+M_N}{\nu+\nu_B}\frac{g_r}{2M_N}\gamma_5\tau_j$$
$$+\text{possible additional pion-pole "seagull" contribution}\Big]u(p_1)\,\psi_j^* + O(q)\ , \tag{40}$$

with

$$\nu = (p_1+p_2)\cdot k/(2M_N)\ ,$$
$$\nu_B = -q\cdot k/(2M_N)\ , \tag{41}$$

and with all other quantities as defined above. The anticommutator term which has appeared in Eq. (40) is the PCAC (partial conservation of axial-vector current) "consistency-condition" term[25] arising from the pseudovector-to-pseudoscalar rearrangement.

With the aid of Eq. (4), we can now proceed to discuss the pion-production model, which is an extension of a calculation of weak pion production in the (3, 3) resonance region which we have described in detail elsewhere.[6] In its original form, the model included the pseudoscalar-coupling Born terms and the pion-pole terms of Eq. (40), with no kinematic approximations. In addition, the dominant (3, 3) multipoles were unitarized by the method used in the CGLN treatment of pion photoproduction,[26] so as to correctly describe (3, 3) resonance excitation. Our basic extended pion-production model is obtained by adding the commutator term in Eq. (40) (evaluated at $q=0$, except where a pion pole appears) and the "consistency-condition" term to the Born approximation and resonant terms of the original model, yielding a pion-production amplitude which has the correct soft-pion limit. In terms of the amplitudes $V_j^{(\pm 0)}$, $j=1,\ldots,6$ and $A_j^{(\pm)}$, $j=1,\ldots,8$ used in Ref. 6 the additions are[27]

$$
\begin{aligned}
\Delta V_1^{(+)} &\approx \frac{g_r}{M_N} F_2^V(k^2) , \\
\Delta V_1^{(0)} &\approx \frac{g_r}{M_N} F_2^S(k^2) , \\
\Delta V_6^{(-)} &\approx \frac{g_r}{M_N} \left[\frac{g_A(k^2)}{g_A} - F_1^V(k^2) \right] (k^2)^{-1} , \\
\Delta A_2^{(-)} &\approx \frac{g_r}{M_N g_A} F_2^V(k^2) , \\
\Delta A_4^{(-)} &\approx - \frac{g_r}{M_N{}^2 g_A} [F_1^V(k^2) - g_A g_A(k^2) \\
&\qquad + 2 M_N F_2^V(k^2)] .
\end{aligned}
\tag{42}
$$

Note that the terms referred to in Ref. 6 as "dispersion-relation corrections to the small partial waves" are omitted from the amplitude, since including them along with the additions of Eq. (42) would involve double counting (and also for the practical reason that the numerical evaluation of the dispersion-relation terms is very costly in terms of computer time).

A further elaboration on the pion-production model consists of adding in the leading corrections (of first order in the pion four-momentum q and zeroth order in the lepton four-momentum transfer k) to the soft-pion limit. These corrections are calculated by the method of Low[28] and Adler and Dothan[28]; for the vector amplitude they vanish (as a result of vector current conservation), while for the isovector axial-vector amplitude they are related by PCAC to momentum derivatives of the pion-nucleon scattering amplitude at the crossing symmetric point. For an isoscalar axial-vector current the $O(q)$ corrections cannot be precisely calculated, but an heuristic resonance dominance argument given in Appendix B suggests that they may be relatively considerably smaller than in the isovector axial-vector case, and so we neglect them. For the isovector axial-vector amplitudes, the calculations of Ref. 28 tell us that[27]

$$
\begin{aligned}
[A_1^{(-)} - A_1^{(-)B}] \,|_0 &\approx \frac{g_A}{g_r} \left. \bar{B}^{\pi N(-)} \right|_{\nu=\nu_B=0} \\
&\quad - \frac{g_r}{2M_N{}^2} \left(\frac{1}{g_A} - g_A + \frac{\mu^V}{g_A} \right) \\
&\approx 0.36 , \\
[A_3^{(+)} - A_3^{(+)B}] \,|_0 &\approx \frac{g_A}{g_r} \left. \frac{\partial \bar{A}^{\pi N(+)}}{\partial \nu_B} \right|_{\nu=\nu_B=0} \\
&\approx 2.8 ; \\
|_0 &\equiv |_{\nu=\nu_B=k^2=0} ,
\end{aligned}
\tag{43a}
$$

with the superscript B indicating the Born approximation and with the numerical values in units in which $M_\pi = 1$. In order to apply Eq. (43a), we must first estimate the extent to which the amplitudes $A_1^{(-)}, A_3^{(+)}$ in our basic pion-production model differ from their Born approximations as a result of unitarization of the (3, 3) multipoles. This is done at the end of Appendix B, with the result

$$
\begin{aligned}
[A_1^{(-)} - A_1^{(-)B}] \,|_0^{\text{basic model}} &\approx 0.21 , \\
[A_3^{(+)} - A_3^{(+)B}] \,|_0^{\text{basic model}} &\approx 0.84 .
\end{aligned}
\tag{43b}
$$

Hence to bring the basic model into agreement with Eq. (43a) we add the $O(q)$ corrections

$$
\begin{aligned}
\Delta A_1^{(-)} &\approx 0.15 (1 + k^2/M^2)^{-2} , \\
\Delta A_3^{(+)} &\approx 1.96 (1 + k^2/M^2)^{-2} .
\end{aligned}
\tag{43c}
$$

Only the $k^2 = 0$ values of the correction terms are actually determined by low-energy theorem arguments; however, to avoid a spurious dominance of these correction terms at large k^2, we have included an *ad hoc* dipole form factor[27] $(1 + k^2/M^2)^{-2}$, characterized by a dipole mass M. In the numerical work of Sec. IV, M was taken equal to the nucleon mass $M_N = 0.94$ GeV, which is rather typical of the dipole mass values[29] found in both the vector and the axial-vector form factors. As we will see in Sec. IV A, substantial variations of M about this value have a relatively small effect on the magnitude of the $O(q)$ corrections to the threshold pion-production cross sections. While the inclusion of the order-q corrections may be an improvement in the amplitude near threshold (or at a minimum, should give an idea of the likely importance of corrections to the basic soft-pion matrix element), their undamped growth as q increases makes their inclusion of doubtful value away from the threshold region. To illustrate this, we also evaluate the $O(q)$ corrections according to the modified recipe

$$
\begin{aligned}
\Delta A_1^{(-)} &\approx (M_N/W)\, 0.15 (1 + k^2/M^2)^{-2} , \\
\Delta A_3^{(+)} &\approx (M_N/W)\, 1.96 (1 + k^2/M^2)^{-2} ,
\end{aligned}
\tag{43d}
$$

which agrees with Eq. (43c) at $\nu = \nu_B = 0$, but which grows less rapidly with increasing W. To sum up, the fully extended pion-production model which we have just described contains both nucleon and pion Born diagrams with no kinematic approximations, includes the dominant (3, 3) multipoles in unitarized form, and agrees with all low-energy-theorem constraints through terms of first order in q and k, with an error of order qk at most. It should thus give a reasonably accurate description of low-invariant-mass pion production, particularly in the region close to invariant-mass threshold.

IV. NUMERICAL RESULTS

We turn now to numerical calculations using the pion-production model developed above. In Sec. IV A we give the results of numerical studies of the model, in which we examine the effect of the $O(q)$ corrections of Eqs. (43c), (43d) and explore their sensitivity to the mass parameter M, and in which we compare the predictions of the model for charged-current-induced neutrino pion production with experiment. In Sec. IV B we use the model to give bounds on the ANL neutral-current-induced threshold pion-production cross section, for a variety of different models for the structure of the weak neutral current. Finally, in Sec. IV C we study low-invariant-mass pion production in the BNL neutrino flux, in the special case of a pure isoscalar weak neutral current.

A. Numerical studies of the model

We begin our numerical examination of the pion-production model of Sec. III C with a study of the $O(q)$ correction terms added to the weak pion production amplitude in Eq. (43). In Table II we give theoretical ANL 2-bin cross sections, defined as in Eq. (16), for the seven allowed charged- and neutral-current-induced pion-production reactions. In column 2 we give the cross section obtained without the $O(q)$ correction [that is, from the basic pion-production model including the soft-pion additions of Eq. (42), but without the additions of Eqs. (43c) or (43d)]. In columns 3, 4, and 5 we give the corresponding cross sections with the $O(q)$ corrections included as in Eq. (43c), taking the *ad hoc* dipole mass M as M_N, $M_N/\sqrt{2}$, and $M_N\sqrt{2}$, respectively. In column 6 we give the cross sections calculated with the $O(q)$ corrections included as in Eq. (43d), with $M=M_N$. We see that the $O(q)$ corrections have a substantial effect on threshold cross sections for $\nu+p\to\nu+p+\pi^0$ and $\nu+n\to\nu+n+\pi^0$, a moderate effect on the cross section for $\nu+p\to\mu^-+p+\pi^+$, and a relatively small effect on the remaining reactions. As expected in the threshold region, the recipes of Eq. (43c) and Eq. (43d) for the $O(q)$ corrections give similar results; we also see that the variation in the threshold cross section as M^2 is changed by a factor of 2 in either direction from $M^2=M_N{}^2$ is smaller than the effect of including the $O(q)$ corrections, indicating that the sensitivity to the value of the mass parameter M is not excessive. In Table III we show the effect of the $O(q)$ additions on the ANL and BNL cross sections integrated over the low-invariant-mass region $W\leq 1.4$ GeV. Again, the reactions $\nu+N\to\nu+N+\pi^0$ are sensitive to the $O(q)$ additions, with the effects on the other cross sections ranging from moderate to small. Here, however, we see a substantial dependence on whether the recipe of Eq. (43c) or of Eq. (43d) is used, indicating that the $O(q)$ additions do not constitute a well-defined correction to the basic pion production model outside the threshold region. A satisfactory treatment of the $O(q)$ terms away from threshold would require their interpretation as the low-energy limits of appropriate particle exchange terms. In the numerical work on the ANL threshold cross sections for $\nu+n\to\nu+p+\pi^-$ described in Sec. IV B, we will include the $O(q)$ correction terms with $M=M_N$. In the numerical work of Sec. IV C analyzing the isoscalar case for the BNL spectrum, we will neglect the $O(q)$ corrections—they vanish for an isoscalar vector current and, as argued in Appendix B, may be relatively small (although hard to estimate precisely) for an isoscalar axial-vector current.

Obviously, the best way to assess the reliability of the pion-production model developed in Sec. III C is to compare its predictions for charged-current-induced pion production reactions with experiment. In Fig. 1 the ANL data[30] for $\nu+p\to\mu^-+p+\pi^+$ are plotted together with predictions

TABLE II. Effect of $O(q)$ additions of Eqs. (43c), (43d) and sensitivity to the *ad hoc* dipole parameter M in the ANL threshold region. Neutral-current cross sections are calculated in the Weinberg-Salam model, with $\sin^2\theta_W=0.35$ and $\Delta\mathfrak{I}^\lambda=0$ [see Eq. (52)].

Reaction	Values of $\sigma_{2\text{ bin}}^{\text{ANL}}$ in 10^{-41} cm^2				
	Without $O(q)$	With $O(q)$ from Eq. (43c) $M=M_N$	$M=M_N/\sqrt{2}$	$M=M_N\sqrt{2}$	With $O(q)$ from Eq. (43d)
$\nu+n\to\mu^-+p+\pi^0$	3.8	3.5	3.6	3.5	3.6
$\nu+p\to\mu^-+p+\pi^+$	4.5	5.9	5.6	6.4	5.7
$\nu+n\to\mu^-+n+\pi^+$	2.3	2.1	2.0	2.2	2.0
$\nu+p\to\nu+p+\pi^0$	0.42	0.73	0.61	0.88	0.64
$\nu+n\to\nu+n+\pi^0$	0.47	0.77	0.65	0.92	0.69
$\nu+n\to\nu+p+\pi^-$	0.91	0.80	0.82	0.77	0.81
$\nu+p\to\nu+n+\pi^+$	0.97	0.87	0.89	0.84	0.88

TABLE III. Effect of $O(q)$ additions of Eqs. (43c), (43d) in the ANL and BNL (3, 3) resonance regions, defined by $W \leq 1.4$ GeV. Neutral-current cross sections are calculated in the Weinberg-Salam model, with $\sin^2\theta_W = 0.35$ and $\Delta\mathcal{G}^\lambda = 0$ [see Eq. (52)]. As is evident from the differences between the two recipes for adding in the $O(q)$ terms away from the threshold region, the $O(q)$ additions do not constitute a well-defined correction to the basic pion production model when the entire (3, 3) resonance region is considered. However, they do usefully indicate which channels may prove to be particularly sensitive to corrections to the basic model.

Reaction	Values of σ^{ANL} ($W \leq 1.4$ GeV) in 10^{-38} cm^2 Without $O(q)$	With $O(q)$ Eq. (43c)	With $O(q)$ Eq. (43d)	Values of σ^{BNL} ($W \leq 1.4$ GeV) in 10^{-38} cm^2 Without $O(q)$	With $O(q)$ Eq. (43c)	With $O(q)$ Eq. (43d)
$\nu+n \to \mu^- + p + \pi^0$	0.0733	0.0694	0.0698	0.147	0.143	0.143
$\nu+p \to \mu^- + p + \pi^+$	0.219	0.237	0.228	0.427	0.499	0.466
$\nu+n \to \mu^- + n + \pi^+$	0.0571	0.0534	0.0491	0.129	0.134	0.116
$\nu+p \to \nu + p + \pi^0$	0.0283	0.0348	0.0308	0.0532	0.0765	0.0629
$\nu+n \to \nu + n + \pi^0$	0.0288	0.0350	0.0311	0.0539	0.0768	0.0634
$\nu+n \to \nu + p + \pi^-$	0.0192	0.0181	0.0181	0.0366	0.0352	0.0351
$\nu+p \to \nu + n + \pi^+$	0.0204	0.0191	0.0192	0.0383	0.0367	0.0367

of the pion production model, both with $O(q)$ additions (curves b and c) and without these additions (curve a). The theoretical curves are evidently low by 30–40% in the case of curve a and by smaller amounts in the cases of curves b and c. Part of this discrepancy may arise from uncertainties in the absolute level of the ANL neutrino flux (these uncertainties are included in the experimental error bars) and in the value of the axial-vector mass parameter[31] M_A, but part is probably due to the known[6] tendency of the pion-production model to underestimate pion-production cross sections for $|k^2| \geq 0.6$ (GeV/c)^2. To minimize this problem, in discussing the BNL isoscalar-current case in Sec. IV C we will always compare *ratios* of cross sections computed within the pion production model with the corresponding ratios obtained experimentally, rather than making direct comparisons of cross sections between theory and experiment. In Table IV we compare preliminary ANL values[32] of the ratios $\sigma(\nu+n \to \mu^- + p + \pi^0)/\sigma(\nu+p \to \mu^- + p + \pi^+)$ and $\sigma(\nu+n \to \mu^- + n + \pi^+)/\sigma(\nu+p \to \mu^- + p + \pi^+)$ with the corresponding theoretical predictions for the invariant-mass interval $W \leq 1.4$ GeV. The agreement is seen to be generally satisfactory. In Fig. 2 we compare the area normalized theoretical invariant-mass distribution for $\nu+p \to \mu^- + p + \pi^+$ [including $O(q)$ corrections from Eq. (43c)] with the corresponding ANL experimental histogram[33]; the agreement in this case is excellent. In Fig. 3 we give the same comparison for the reactions[34] $\nu+n \to \mu^- + p + \pi^0$ and $\nu+n \to \mu^- + n + \pi^+$. The agreement is again satisfactory. In general, the comparisons given above suggest that the pion-production model developed in Sec. III C should be reliable to better than a factor of 2 in the region at and below resonance. The reliability should be substantially better than this for relative cross-section ratios or reactions without large $O(q)$ corrections.

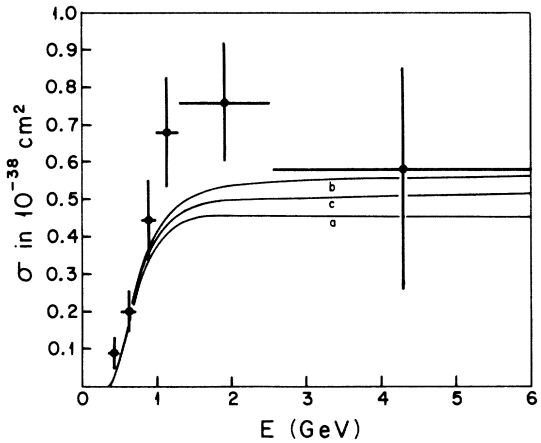

FIG. 1. Comparison of the extended pion-production model of Sec. III C with the ANL data for $\nu + p \to \mu^- + p + \pi^+$. Curve a, basic model containing Born, resonant, and soft-pion terms; curve b, basic model with $O(q)$ additions from Eq. (43c); curve c, basic model with $O(q)$ additions from Eq. (43d).

B. Threshold neutral-current-induced pion production in the ANL flux

We consider now the application of the formulas developed in Sec. III to the study of neutral-cur-

TABLE IV. Comparison of theoretical predictions for charged-current pion final-state ratios with preliminary ANL experimental results (Ref. 32).

Ratio	Experiment	Theory Without $O(q)$	Theory With $O(q)$ Eq. (43c)	Theory With $O(q)$ Eq. (43d)
$\frac{\sigma(\nu+n\to\mu^-+p+\pi^0)}{\sigma(\nu+p\to\mu^-+p+\pi^+)}$	0.27 ± 0.06	0.34	0.29	0.31
$\frac{\sigma(\nu+n\to\mu^-+n+\pi^+)}{\sigma(\nu+p\to\mu^-+p+\pi^+)}$	0.31 ± 0.07	0.26	0.23	0.22

rent-induced threshold pion production in the ANL neutrino flux.[4] We start with the general six-parameter neutral-current structure in Eq. (18), but we note that since the isoscalar axial currents contribute only[35] through the $g_A^{(0,8)}\gamma^\lambda\gamma_5$ term in their nucleon vertices, the effective number of parameters entering the pion production calculation can be reduced to 5. These are conveniently introduced by writing the one-nucleon matrix element of the neutral current as

$$\langle N(p_2)|\mathcal{J}_N^\lambda|N(p_1)\rangle = \mathfrak{N}_N\bar{u}(p_2)\{[-\lambda_1 g_A(k^2)\gamma^\lambda\gamma_5+\lambda_2 F_1^V(k^2)\gamma^\lambda+i\lambda_2 F_2^V(k^2)\sigma^{\lambda\eta}k_\eta]\tfrac{1}{2}\tau_3$$
$$+[-\lambda_3 D(k^2)\gamma^\lambda\gamma_5+\lambda_4 D(k^2)\gamma^\lambda+i\lambda_5(2M_N)^{-1}D(k^2)\sigma^{\lambda\eta}k_\eta]\tfrac{1}{2}\}u(p_1)\ , \tag{44}$$

with $D(k^2)$ a dipole structure characterizing the isoscalar current vertices, which for definiteness we take as

$$D(k^2)=(1-k^2/M_N^2)^{-2}\ . \tag{45}$$

To a first approximation, we expect[36] that small changes in the isoscalar dipole mass parameter from the assigned value of M_N can be compensated by making appropriate rescalings of the isoscalar parameters $\lambda_{3,4,5}$. In terms of the parameters $\lambda_1,\ldots,\lambda_4$, the couplings $g_{V_{0,3,8}}, g_{A_{0,3,8}}$ introduced in Eq. (18) are given by

$$g_{V_0}(\tfrac{2}{3})^{1/2}+g_{V_8}(\tfrac{1}{3})^{1/2}=\tfrac{1}{3}\lambda_4,\quad g_{V_3}=\lambda_2\ ,$$
$$g_{A_0}(\tfrac{2}{3})^{1/2}+g_{A_8}(\tfrac{1}{3})^{1/2}=\frac{1}{g_A^S}\lambda_3,\quad g_{A_3}=\lambda_1\ , \tag{46a}$$

with g_A^S an effective isoscalar axial-vector renormalization constant defined by

$$g_A^S=\frac{g_{A_0}(\frac{2}{3})^{1/2}g_A^{(0)}(0)+g_{A_8}(\frac{1}{3})^{1/2}g_A^{(8)}(0)}{g_{A_0}(\frac{2}{3})^{1/2}+g_{A_8}(\frac{1}{3})^{1/2}}\ . \tag{46b}$$

In terms of these definitions, the deep-inelastic constraint of Eq. (36) becomes

$$1.5\geq 3R_\nu+R_{\bar\nu}\geq\lambda_1^2+\lambda_2^2, \tag{47}$$

while the stronger constraint of Eq. (37), which follows when quark-parton-model information is used, takes the form

$$1.5\geq 3R_\nu+R_{\bar\nu}=\lambda_1^2+\lambda_2^2+\frac{\lambda_3^2}{(g_A^S)^2}+\tfrac{1}{9}\lambda_4^2. \tag{48}$$

Equations (15) and (47), or (15) and (48), are the basic constraints which will be imposed in maximizing $\sigma_{2\text{bin}}^{\text{ANL}}$ over the space of parameters $\lambda_1,\ldots,\lambda_5$.

Obviously, to recompute the pion-production and neutrino-proton–elastic-scattering cross sections for each distinct set of parameter values being studied would be a very inefficient procedure from

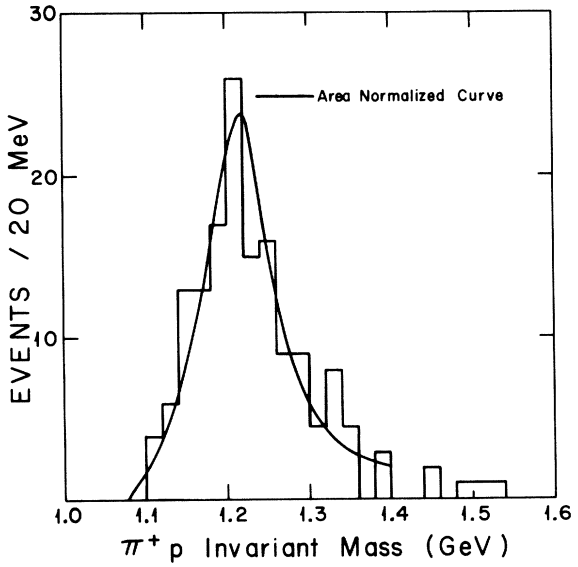

FIG. 2. Comparison of the area-normalized theoretical invariant-mass distribution for $\nu+p\to\mu^-+p+\pi^+$ [calculated with $O(q)$ additions from Eq. (43c)] with the ANL histogram for this reaction.

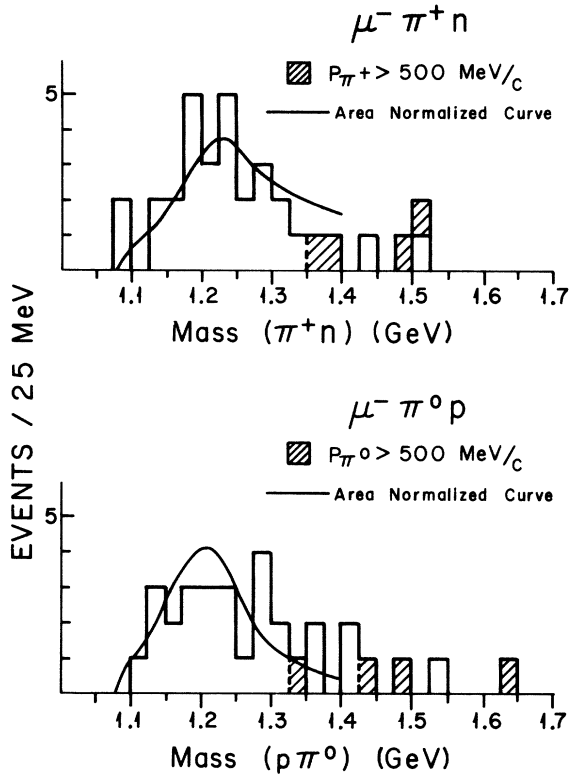

FIG. 3. Comparison of the area-normalized theoretical invariant-mass distributions for $\nu + n \to \mu^- + n + \pi^+$ and $\nu + n \to \mu^- + p + \pi^0$ [calculated with $O(q)$ additions from Eq. (43c)] with the corresponding ANL histograms. The theoretical predictions have been folded with the experimental invariant-mass resolutions of 25 MeV for $n + \pi^+$ and 40 MeV for $p + \pi^0$.

a numerical point of view. Rather, we exploit the fact that the cross sections are quadratic forms in the parameters λ_j, taking the form

$$\sigma_{2\,\mathrm{bin}}^{\mathrm{ANL}}/10^{-38}\ \mathrm{cm}^2 = \sum_{i=1}^{5} \sum_{1\le j\le i} P_{ij}\lambda_i\lambda_j,$$
$$\sigma^{\mathrm{ANL}}(\nu + p \to \nu + p)/10^{-38}\ \mathrm{cm}^2 = \sum_{i=1}^{5} \sum_{1\le j\le i} E_{ij}\lambda_i\lambda_j, \tag{49}$$

so it is only necessary to perform the cross-section calculation for the 15 parameter sets

$$\left.\begin{aligned} &\lambda_i = 0, \quad i \neq I, J \\ &\lambda_I = 1, \quad \lambda_J = 1 \end{aligned}\right\} \quad 1 \le I \le J \le 5 \tag{50}$$

to extract the coefficients[4] P_{ij}, E_{ij}, which are tabulated in Table V. The quadratic forms of Eq. (49) are then used to compute the cross sections when searching over parameter values, permitting a complete survey of the five-parameter space using a very reasonable amount of computer time.

TABLE V. Coefficients determining $\sigma_{2\,\mathrm{bin}}^{\mathrm{ANL}}$ and $\sigma^{\mathrm{ANL}}(\nu + p \to \nu + p)$ via the quadratic forms of Eq. (49). Note the comment in Ref. 4.

Pion-production coefficients		Elastic-scattering coefficients	
P_{11}	0.621×10^{-3}	E_{11}	0.692×10^{-1}
P_{22}	0.807×10^{-3}	E_{22}	0.767×10^{-1}
P_{33}	0.163×10^{-3}	E_{33}	0.478×10^{-1}
P_{44}	0.244×10^{-4}	E_{44}	0.364×10^{-1}
P_{55}	0.121×10^{-4}	E_{55}	0.300×10^{-2}
P_{12}	0.534×10^{-3}	E_{12}	0.656×10^{-1}
P_{13}	0.772×10^{-5}	E_{13}	0.115
P_{14}	0.166×10^{-4}	E_{14}	0.158×10^{-1}
P_{15}	-0.211×10^{-4}	E_{15}	0.159×10^{-1}
P_{23}	-0.393×10^{-4}	E_{23}	0.554×10^{-1}
P_{24}	0.143×10^{-3}	E_{24}	0.858×10^{-1}
P_{25}	-0.312×10^{-4}	E_{25}	0.201×10^{-1}
P_{34}	0.328×10^{-4}	E_{34}	0.134×10^{-1}
P_{35}	0.532×10^{-4}	E_{35}	0.134×10^{-1}
P_{45}	0.996×10^{-5}	E_{45}	0.229×10^{-2}

The results, for various assumptions about the structure of the weak neutral current, are as follows:

(1) Pure isoscalar weak neutral current. Taking $\lambda_1 = \lambda_2 = 0$ and maximizing $\sigma_{2\,\mathrm{bin}}^{\mathrm{ANL}}$ over the $\lambda_3, \lambda_4, \lambda_5$ subspace subject to the constraint of Eq. (15) gives the upper bound

$$\sigma_{2\,\mathrm{bin}}^{\mathrm{ANL}} \le 1.0\times10^{-41}\ \mathrm{cm}^2. \tag{51}$$

(2) Weinberg-Salam SU(2)⊗U(1) model. In the simplest, one-parameter version of this model,[37] the neutral current has the form

$$\mathcal{J}_N^\lambda = \mathfrak{F}_3^\lambda - \mathfrak{F}_3^{5\lambda} - 2x(\mathfrak{F}_3^\lambda + 3^{-1/2}\mathfrak{F}_8^\lambda) + \Delta\mathcal{J}^\lambda,$$
$$x = \sin^2\theta_W, \tag{52}$$

with $\Delta\mathcal{J}^\lambda$ an isoscalar $V-A$ strangeness and "charm" current contribution which is conventionally assumed to couple only weakly to nonstrange low-mass hadrons (such as the low-energy pion-nucleon system). Neglecting $\Delta\mathcal{J}^\lambda$ for the moment we can make an absolute calculation of the cross section for $\nu + n \to \nu + p + \pi^-$, giving

$$\sigma_{2\,\mathrm{bin}}^{\mathrm{ANL}} = 0.75\times10^{-41}\ \mathrm{cm}^2. \tag{53}$$

In certain extensions of the original Weinberg-Salam model, the neutral current has the general form of Eq. (52), but with an adjustable strength parameter κ in front,

$$\mathcal{J}_N^\lambda = \kappa[\mathfrak{F}_3^\lambda - \mathfrak{F}_3^{5\lambda} - 2x(\mathfrak{F}_3^\lambda + 3^{-1/2}\mathfrak{F}_8^\lambda)] + \Delta\mathcal{J}^\lambda. \tag{54}$$

Still neglecting $\Delta\mathcal{J}^\lambda$, and comparing with Eq. (44), we now see that the parameters λ_j have the values

$$\lambda_1 = \kappa,$$
$$\lambda_2 = \kappa(1-2x), \quad \lambda_4 = -2\kappa x, \tag{55}$$
$$\lambda_3 = 0. \qquad \lambda_5 = 0.24\kappa x.$$

Maximizing $\sigma_{2\,\mathrm{bin}}^{\mathrm{ANL}}$ over the κ, x parameter space (allowing all real values of x, rather than restricting x to lie between 0 and 1) subject to the constraints of Eqs. (15) and (47) gives the upper bound

$$\sigma_{2\,\mathrm{bin}}^{\mathrm{ANL}} \leq 1.5\times 10^{-41}\ \mathrm{cm}^2. \tag{56}$$

Finally, we can include the isoscalar addition $\Delta\mathcal{J}^\lambda$ by regarding $\lambda_3, \lambda_4, \lambda_5$ as free parameters, rather than relating them to κ and x as in Eq. (55). Searching now over the five-parameter $\kappa, x, \lambda_3, \lambda_4, \lambda_5$ space (again allowing all real values of x) subject to the constraints of Eqs. (15) and (47) gives the upper bound

$$\sigma_{2\,\mathrm{bin}}^{\mathrm{ANL}} \leq 4.6\times 10^{-41}\ \mathrm{cm}^2. \tag{57}$$

We emphasize that Eq. (57) *is the upper bound on* $\sigma_{2\,\mathrm{bin}}^{\mathrm{ANL}}$ *for the most general hadronic neutral current formed from the usual vector and axial-vector nonets*. If Eq. (47) is replaced by the stronger constraint of Eq. (48), and if the parameters $g \equiv \lambda_5/\lambda_4$ and g_A^S are restricted [as suggested by the quark-model[16,24] values of Eq. (39)] by

$$|g| \leq 1.5, \quad |g_A^S| \leq 0.74, \tag{58}$$

then the bound in the general V,A case is substantially reduced, to

$$\sigma_{2\,\mathrm{bin}}^{\mathrm{ANL}} \leq 1.5\times 10^{-41}\ \mathrm{cm}^2. \tag{59}$$

C. Analysis of low-invariant-mass ($W \leq 1.4$ GeV) pion production at BNL: Isoscalar current case

We turn finally to an analysis of low-invariant-mass ($W \leq 1.4$ GeV) pion production in the BNL neutrino flux.[38] Recently, the Columbia-Illinois-Rockefeller collaboration at BNL has reported a measurement of the ratio

$$R_0' = \frac{\sigma(\nu + T \to \nu + \pi^0 + \cdots)}{2\sigma(\nu + T \to \mu^- + \pi^0 + \cdots)}, \qquad T = \tfrac{1}{4}(_6C^{12}) + \tfrac{3}{4}(_{13}Al^{27}), \tag{60}$$

with the preliminary result[3,39]

$$R_0' = 0.17 \pm 0.06. \tag{61}$$

This measured value of R_0' is in accord with the value expected[40] in the Weinberg-Salam model when $\sin^2\theta_W$ is in the currently favored range of 0.3–0.4. Hence *if* (3, 3) resonance excitation, which is expected in the Weinberg-Salam model (see Fig. 4), is observed in the BNL experiment, the presumption would be strongly in favor of the standard gauge-theory interpretation of neutral currents. However, preliminary BNL invariant-mass spectra[3] for π^0 production in the charged- and neutral-current cases show a clear (3, 3) peak in the charged-current case, but indicate no comparable peaking in the neutral-current reaction, suggesting that perhaps the (3, 3) resonance is not excited by the neutral current. In what follows we analyze the implications for neutral-current structure if this indication is confirmed both by more detailed analysis of the BNL data and by other experiments.

Since the isovector V and A neutral currents both[41] strongly excite the (3, 3) resonance, the absence of a (3, 3) peak in the V,A case would suggest an isoscalar neutral-current structure, and we assume this in what follows. Applying nuclear charge-exchange corrections as described in Appendix C, we find that the nuclear target ratio quoted in Eq. (61) implies the free-nucleon target ratio

$$2R_0 \equiv \frac{\sigma^{\mathrm{BNL}}(\nu + n \to \nu + n + \pi^0) + \sigma^{\mathrm{BNL}}(\nu + p \to \nu + p + \pi^0)}{\sigma^{\mathrm{BNL}}(\nu + n \to \mu^- + p + \pi^0)} = 2R_0' \times 1.4 = 0.48 \pm 0.17. \tag{62}$$

Let us now compare the experimental result of Eq. (62) with theoretical predictions obtained from the extended pion production model developed in

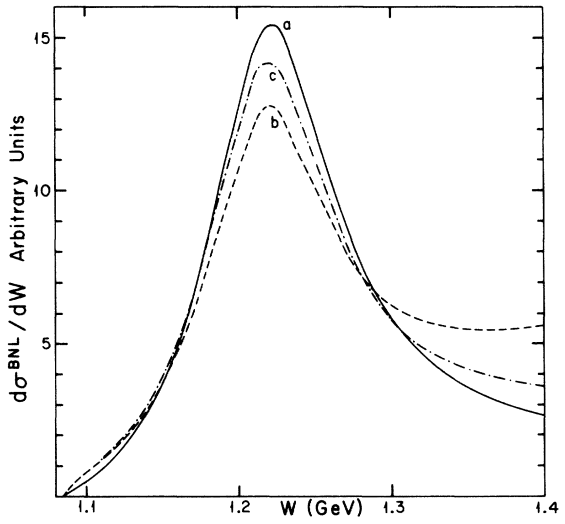

FIG. 4. Area-normalized, BNL-flux-averaged theoretical invariant-mass distribution in the Weinberg-Salam model (with $\sin^2\theta_W = 0.35$) for the reaction $\nu + p \to \nu + p + \pi^0$. Curve a, basic model containing Born, resonant, and soft-pion terms; curve b, basic model with $O(q)$ additions from Eq. (43c); curve c, basic model with $O(q)$ additions from Eq. (43d).

Sec. III C, in the case of a pure isoscalar neutral current. Again we parameterize the neutral current as in Eq. (44), with $\lambda_1 = \lambda_2 = 0$. The BNL flux-averaged pion production and elastic cross sections are then quadratic forms in $\lambda_3, \lambda_4, \lambda_5$, taking the form

$$[\sigma^{\mathrm{BNL}}(\nu + n \to \nu + n + \pi^0,\ W \le W_M) + \sigma^{\mathrm{BNL}}(\nu + p \to \nu + p + \pi^0,\ W \le W_M)]/10^{-38}\ \mathrm{cm}^2 = \sum_{i=3}^{5} \sum_{3 \le j \le i} P_{ij}(W_M)\lambda_i\lambda_j,$$

$$\sigma^{\mathrm{BNL}}(\nu + p \to \nu + p,\ \text{Cundy cuts})/10^{-38}\ \mathrm{cm}^2 = \sum_{i=3}^{5} \sum_{3 \le j \le i} E_{ij}^{(1)}\lambda_i\lambda_j,$$

$$\sigma^{\mathrm{BNL}}(\nu + p \to \nu + p,\ \text{no cuts})/10^{-38}\ \mathrm{cm}^2 = \sum_{i=3}^{5} \sum_{3 \le j \le i} E_{ij}^{(2)}\lambda_i\lambda_j; \tag{63}$$

Cundy cuts: $1\ \mathrm{GeV} \le E \le 4\ \mathrm{GeV}$, $0.3\ (\mathrm{GeV}/c)^2 \le |k^2| \le 1\ (\mathrm{GeV}/c)^2$.

The pion-production coefficients P_{ij} (for $W_M = 1.2$, 1.3, and 1.4 GeV) and the cut and uncut[42] elastic-scattering coefficients E_{ij} required in Eq. (63) are tabulated in Table VI. In maximizing the pion-production cross section over the space of parameters $\lambda_3, \lambda_4, \lambda_5$, we impose the constraints

$$\sigma^{\mathrm{BNL}}(\nu + p \to \nu + p,\ \text{Cundy cuts}) \le 0.24\sigma^{\mathrm{BNL}}(\nu + n \to \mu^- + p,\ \text{Cundy cuts}) \approx 0.085 \times 10^{-38}\ \mathrm{cm}^2,$$
$$1.5 \ge 3R_\nu + R_{\bar\nu} = \frac{\lambda_3^2}{(g_A^S)^2} + \tfrac{1}{9}\lambda_4^2, \tag{64}$$

the first of which is the Cundy *et al.*[43] 95% confidence-level limit from the CERN neutrino experiment, which has a neutrino flux similar[43] to that of the BNL experiment, while the second is the deep-inelastic quark-parton-model constraint of Eqs. (37) and (48) above. The results of the maximization are expressed as theoretical upper bounds on the ratio $2R_0$ defined in Eq. (62), with *both* the numerator and the denominator calculated from the pion production model. As stressed in Sec. IV A, the procedure of comparing theoretical cross-section *ratios* with experimental ratios should minimize the effects of discrepancies between the experimental and theoretical cross-section magnitudes. For the denominator cross section $\sigma^{\mathrm{BNL}}(\nu + n \to \mu^- + p + \pi^0,\ W \le 1.4\ \mathrm{GeV})$ we use the value $0.143 \times 10^{-38}\ \mathrm{cm}^2$ listed in columns 6 and 7 of Table III, corresponding to inclusion of $O(q)$ corrections; however, as is apparent from the table, the effect of the $O(q)$ corrections on this cross section is very small.

Results of the maximization calculation[44] are given in Figs. 5 and 6. Curve a of Fig. 5 gives the maximum for an isoscalar pure vector current, while curve b gives the maximum when an octet isoscalar axial-vector current is also present (corresponding to $g_A^S = 0.45$), both plotted versus the isoscalar current gyromagnetic ratio $g = \lambda_5/\lambda_4$. Evidently, both curves lie below the BNL data, with a discrepancy exceeding a factor of 2 unless $|g| \gtrsim 4$–6, that is, unless the isoscalar vector current has a $|g|$ value which is anomalously large based on quark-model expectations.[24] Interestingly, a vector current with a large $|g|$ value pro-

TABLE VI. Coefficients determining $\sigma^{\mathrm{BNL}}(\nu + n \to \nu + n + \pi^0) + \sigma^{\mathrm{BNL}}(\nu + p \to \nu + p + \pi^0)$ for various W ranges and $\sigma^{\mathrm{BNL}}(\nu + p \to \nu + p)$, both cut and uncut, via the quadratic forms of Eq. (63).

	Pion-production coefficients			Elastic-scattering coefficients			
	$W \le 1.2$ GeV	$W \le 1.3$ GeV	$W \le 1.4$ GeV		Cundy cuts		No cuts
P_{33}	0.210×10^{-2}	0.607×10^{-2}	0.109×10^{-1}	$E_{33}^{(1)}$	0.176×10^{-1}	$E_{33}^{(2)}$	0.555×10^{-1}
P_{44}	0.286×10^{-3}	0.638×10^{-3}	0.994×10^{-3}	$E_{44}^{(1)}$	0.158×10^{-1}	$E_{44}^{(2)}$	0.515×10^{-1}
P_{55}	0.193×10^{-3}	0.566×10^{-3}	0.106×10^{-2}	$E_{55}^{(1)}$	0.265×10^{-2}	$E_{55}^{(2)}$	0.480×10^{-2}
P_{34}	0.247×10^{-3}	0.925×10^{-3}	0.165×10^{-2}	$E_{34}^{(1)}$	0.558×10^{-2}	$E_{34}^{(2)}$	0.105×10^{-1}
P_{35}	0.467×10^{-3}	0.138×10^{-2}	0.258×10^{-2}	$E_{35}^{(1)}$	0.558×10^{-2}	$E_{35}^{(2)}$	0.105×10^{-1}
P_{45}	0.169×10^{-3}	0.519×10^{-3}	0.941×10^{-3}	$E_{45}^{(1)}$	0.635×10^{-3}	$E_{45}^{(2)}$	0.142×10^{-2}

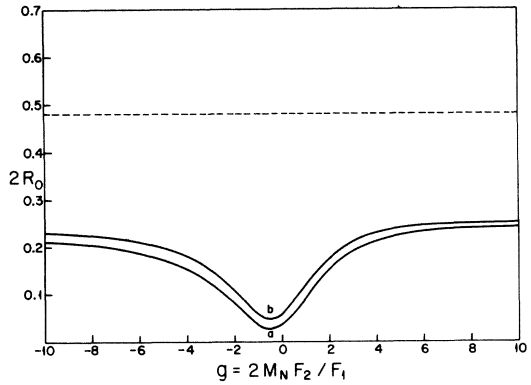

FIG. 5. Results of a maximization calculation for BNL cross-section ratios in the invariant-mass interval $W \leq 1.4$ GeV, plotted versus the g value of the isoscalar vector current. Curve a is the maximum for an isoscalar pure vector current; curve b is the maximum when an isoscalar axial current is also present, with the axial-vector renormalization constant fixed at $g_A^S = 0.45$ (the octet axial-vector current value). The dashed line is the central experimental value from Eq. (62).

duces a characteristic change in the $d\sigma/dW$ plot predicted for the BNL flux, as shown in the dashed curve in Fig. 7. [The dashed curve is calculated for the case of an isoscalar vector current containing only an F_2 form factor; for the F_1, F_2 admixture corresponding to $|g| = 4$, the curve is substantially the same. Similarly, changing the *ad hoc* dipole mass in Eq. (45) from M_N to $M_N\sqrt{2}$ or

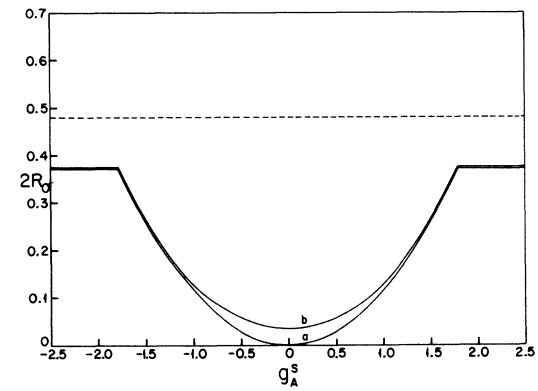

FIG. 6. Results of a maximization calculation for BNL cross-section ratios in the invariant-mass interval $W \leq 1.4$ GeV, plotted versus the effective renormalization constant g_A^S of the isoscalar axial-vector current. Curve a is the maximum for an isoscalar pure axial-vector current; curve b is the maximum when an isoscalar vector current is also present, with g value fixed at -0.12 (the quark model and octet vector current value). The dashed line is the central experimental value from Eq. (62).

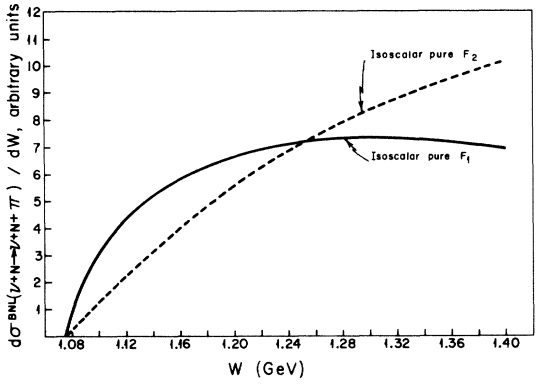

FIG. 7. Shapes of $d\sigma/dW$ for an isoscalar vector current containing an F_1 term only or an F_2 term only. The two curves are normalized to equal area for $W \leq 1.4$ GeV.

$M_N/\sqrt{2}$ produces only a 2% change in the dashed curve.] As seen in the figure, an isoscalar vector current with large $|g|$ produces, relative to the pure F_1 case,[45] a depression in the $d\sigma/dW$ distribution for small W, characterized by an almost linear rise from threshold, and a corresponding enhancement at the large W end of the range. An experiment with good statistics should be able to search for this effect. Continuing with the results of the maximization calculation, curve a of Fig. 6 gives the maximum for an isoscalar pure axial-vector current, while curve b gives the maximum when an isoscalar vector current is also present (with gyromagnetic ratio fixed at the quark-model value of -0.12), both plotted versus the effective axial-vector renormalization constant g_A^S. Deviation of g_A^S from the octet value of 0.45 of course requires the presence of a contribution from the SU(3)-singlet axial-vector current. The curves again lie below the BNL data, with a discrepancy exceeding a factor of 2 unless $|g_A^S| \gtrsim 1.5$, which would imply a sizable ninth axial-vector current contribution and a relatively large ninth current renormalization constant as compared with quark-model expectations.[24]

To summarize, if the observed BNL neutral-current pion production rate is to be interpreted in terms of isoscalar V, A currents, then existing elastic and deep-inelastic constraints require that the neutral current contain either a vector current with anomalously large $|g|$ value, or an appreciable coupling to the ninth [SU(3) singlet] axial-vector current.

We conclude by briefly mentioning two other qualitative features of an isoscalar V, A neutral current which may help to distinguish it from alternative phenomenological neutral-current struc-

tures. First, referring to Table VI we note that the V,A interference terms in νp elastic scattering and in weak pion production (for $W \leq 1.4$ GeV) are given by

elastic scattering:

$$V,A \text{ interference} \propto (\text{positive}) \times \lambda_3\lambda_4(1+g),$$

weak pion production: (65)

$$V,A \text{ interference} \propto (\text{positive}) \times \lambda_3\lambda_4(0.64+g),$$

$$g = \lambda_5/\lambda_4.$$

Hence, except for the small range of isoscalar gyromagnetic ratios

$$-1 \leq g \leq -0.64, \tag{66}$$

the interference terms in neutral-current elastic νp scattering and weak pion production have the same sign. That is, except for g values in the range of Eq. (66), constructive V,A interference in $\nu + N \to \nu + N + \pi$ implies constructive interference in $\nu + p \to \nu + p$ and vice versa. A second useful remark (which has been made by many authors) is that if ν and $\bar{\nu}$ neutral-current cross sections differ (implying the presence of V,A interference effects in a V,A current picture), then the neutral interaction may induce parity-violating terms in the pp, ep, and μp interactions. The significance of this statement is that the same connection between $\nu, \bar{\nu}$ cross-section differences and parity-violating effects does not hold in other neutral-current phenomenologies, such as the S,P,T current picture to be discussed in the second paper[5] of this series.

ACKNOWLEDGMENTS

I wish to thank S. F. Tuan for stimulating discussions about the structure of neutral currents, S. B. Treiman for many helpful critical comments in the course of this work, and members of the Argonne-Purdue collaboration and of the Columbia-Illinois-Rockefeller collaboration for conversations about the Argonne and Brookhaven neutrino experiments. Initial parts of this work were done while I was a visitor at the National Accelerator Laboratory; I am grateful to Professor B. W. Lee for the hospitality of the theory group there. I wish also to thank Y. J. Ng for checking the calculation of Appendix B, and H. Frauenfelder, M. L. Goldberger, E. Henley, V. Hughes, J. J. Sakurai, F. J. Wilczek, and L. Wolfenstein for useful remarks.

APPENDIX A

We give here the analog of the low-energy theorem of Eq. (12) for the case of the SU(2) $\otimes$ U(1)-model neutral current of Eq. (52), with $\Delta\mathcal{J}^\lambda = 0$. (The following formulas still neglect the pion mass in the kinematics and so were not used in the numerical work described in the text.) The threshold pion production cross section is given by

$$\frac{1}{|\vec{q}|}\frac{d\sigma(\nu+N\to\nu+N+\pi)}{dt\,dW}\bigg|_{\text{threshold}} = \frac{G^2}{16\pi^3}\frac{1}{E^2}\left(\frac{g_r}{2M_N{}^2}\right)^2\left(1+\frac{t}{4M_N{}^2}\right)\left(1+\frac{t}{2M_N{}^2}\right)^{-2}\hat{T},$$

$$\hat{T} = (2M_N{}^2)^{-1}\left[\left(1+\frac{t}{4M_N{}^2}\right)^{-1}(H_1{}^2+tH_2{}^2)+(H_4{}^2+tH_3{}^2)\right][4M_N{}^2E^2 - t(M_N{}^2+2M_NE)]$$

$$+t\left[H_1{}^2+t\left(1+\frac{t}{4M_N{}^2}\right)H_3{}^2\right]+\xi H_1H_3\frac{t}{M_N}(4M_NE-t), \tag{A1}$$

with $\xi = 1$ (-1) for ν $(\bar{\nu})$-induced reactions, and with

$$H_1 = a_E^{(-)}(1-2x)2M_N\left(1+\frac{t}{2M_N{}^2}\right)\frac{g_A(k^2)}{g_A}+\frac{t}{2M_N}[\hat{F}_1(k^2)+2M_N\hat{F}_2(k^2)],$$

$$H_2 = -\hat{F}_1(k^2)+\frac{t}{2M_N}\hat{F}_2(k^2),$$

$$H_3 = a_E^{(-)}\frac{1}{g_A}[F_1^V(k^2)+2M_NF_2^V(k^2)]\frac{1+t/2M_N{}^2}{1+t/4M_N{}^2}+\hat{g}_A(k^2),$$

$$H_4 = a_E^{(-)}\frac{2M_N}{g_A}\frac{(1+t/2M_N{}^2)}{(1+t/4M_N{}^2)}\left[F_1^V(k^2)-\frac{t}{2M_N}F_2^V(k^2)\right], \tag{A2}$$

$$\hat{F}_{1,2}(k^2) = F_{1,2}^V(k^2)[a_E^{(+)}-a_E^{(-)}](1-2x)+F_{1,2}^S(k^2)a_E^{(0)}(-2x),$$

$$\hat{g}_A(k^2) = g_A(k^2)[a_E^{(+)}-a_E^{(-)}].$$

TABLE VII. Isospin coefficients appearing in Eq. (A2).

	$a_E^{(+)}$	$a_E^{(-)}$	$a_E^{(0)}$
$\begin{pmatrix}\nu\\ \bar{\nu}\end{pmatrix}+p\to\begin{pmatrix}\nu\\ \bar{\nu}\end{pmatrix}+p+\pi^0$	$\frac{1}{2}$	0	$\frac{1}{2}$
$\begin{pmatrix}\nu\\ \bar{\nu}\end{pmatrix}+n\to\begin{pmatrix}\nu\\ \bar{\nu}\end{pmatrix}+n+\pi^0$	$\frac{1}{2}$	0	$-\frac{1}{2}$
$\begin{pmatrix}\nu\\ \bar{\nu}\end{pmatrix}+n\to\begin{pmatrix}\nu\\ \bar{\nu}\end{pmatrix}+p+\pi^-$	0	$-\frac{1}{\sqrt{2}}$	$\frac{1}{\sqrt{2}}$
$\begin{pmatrix}\nu\\ \bar{\nu}\end{pmatrix}+p\to\begin{pmatrix}\nu\\ \bar{\nu}\end{pmatrix}+n+\pi^+$	0	$\frac{1}{\sqrt{2}}$	$\frac{1}{\sqrt{2}}$

As in the text, we have used the abbreviations $t=-k^2$, $x=\sin^2\theta_W$. The isospin coefficients $a_E^{(\pm 0)}$ are given in Table VII. As the diligent reader may verify, in the case of π^0 production (for which the low-energy-theorem equal-time commutator vanishes) Eqs. (A1) and (A2) reduce to Eq. (12) of the text, with $d\sigma(\nu+N\to\nu+N)/dt$ appropriate to the Weinberg-Salam-model case of Eqs. (21)–(23). Since Eqs. (A1) and (A2) were obtained by algebraic reduction from the Born-approximation expressions of Ref. 6, this agreement provides a cross check on the extended pion-production model of Sec. III C.

APPENDIX B

We give first a rough estimate of the $O(q)$ corrections in the case of an isoscalar octet axial-vector current. We start from the analogy $\pi^0 \leftrightarrow$ SU(3)-3 index, $\eta \leftrightarrow$ SU(3)-8 index and the fact that $A^{\pi N(+)}=\bar{A}^{\pi^0 N\to\pi^0 N}$, which allows us to write[46] (in units with $M_\pi=1$)

Isovector:

$$\Delta A_3^{(+)}=\frac{g_A}{g_r}\frac{\partial}{\partial\nu_B}A^{\pi^0 N\to\pi^0 N}\Big|_0\approx 2.8\,, \tag{B1}$$

Octet isoscalar:

$$\Delta A_3^{(\eta)}=\frac{g_A^{(\eta)}}{g_r^{(\eta)}}\frac{\partial}{\partial\nu_B}A^{\pi^0 N\to\eta N}\Big|_0\,.$$

Here g_r and $g_r^{(\eta)}$ are, respectively, the $\pi^0 NN$ and the ηNN coupling constants, which according to octet PCAC and SU(3) are related by

$$\frac{g_r^{(\eta)}}{g_r}=\frac{g_A^{(\eta)}}{g_A}\approx\frac{3-(4\times 0.66)}{\sqrt{3}}=0.21\,. \tag{B2}$$

Since the over-all magnitudes of the leading terms in the axial-vector soft-pion amplitude in the isovector and the octet isoscalar cases are governed respectively by g_A and $g_A^{(\eta)}$, a convenient measure of the importance of the $O(q)$ correction in the isoscalar octet axial-vector case, relative to its importance in the isovector axial-vector case, is given by

$$R\equiv\frac{\Delta A_3^{(\eta)}/g_A^{(\eta)}}{\Delta A_3^{(+)}/g_A}=0.16\,\frac{\partial}{\partial\nu_B}A^{\pi^0 N\to\eta N}\Big|_0\,. \tag{B3}$$

To estimate the derivative appearing in Eq. (B3), we assume an unsubtracted dispersion relation[47]

$$A^{\pi^0 N\to\eta N}=\frac{1}{\pi}\int_{x_0}^{\infty}dx'\left(\frac{1}{x'-x}+\frac{1}{x'+x+2\nu_B}\right)\times\operatorname{Im}A^{\pi^0 N\to\eta N}\,,\qquad x^0=M_\pi+M_\pi^2/(2M_N)\,. \tag{B4}$$

We approximate the integral by supposing $A^{\pi^0 N\to\eta N}$ to be dominated by those partial waves containing resonances which couple $\pi^0 N$ strongly to ηN. Referring to the Particle Data Group summary,[48] we see that the only such resonances are the $N^*(1535)$ ($J^P=\frac{1}{2}^-$) and the $N^*(1470)$ ($J^P=\frac{1}{2}^+$). Writing the partial-wave expansion for $A^{\pi^0 N\to\eta N}$ and keeping only the f_{0+} and f_{1-} partial waves to which the $N^*(1535)$ and $N^*(1470)$ respectively contribute, we find[49]

$$\operatorname{Im}A^{\pi^0 N\to\eta N}=\frac{4\pi(W+M_N)\operatorname{Im}f_{0+}^{\pi^0 N\to\eta N}}{[(p_{10}+M_N)(p_{20}+M_N)]^{1/2}}-\frac{4\pi(W-M_N)\operatorname{Im}f_{1-}^{\pi^0 N\to\eta N}}{[(p_{10}-M_N)(p_{20}-M_N)]^{1/2}}\,, \tag{B5}$$

which is independent of ν_B. So in the approximation of dominance by the $N^*(1535)$ and $N^*(1470)$, we have

$$\frac{\partial}{\partial\nu_B}\operatorname{Im}A^{\pi^0 N\to\eta N}=0\,. \tag{B6}$$

Hence, only the derivative of the explicit ν_B in Eq. (B4) contributes, and we find

$$\frac{\partial}{\partial\nu_B}A^{\pi^0 N\to\eta N}\Big|_0\approx-\frac{2}{\pi}\int_{x_0}^{\infty}\frac{dx'}{(x')^2}\operatorname{Im}A^{\pi^0 N\to\eta N}(x',\nu_B=0)\,. \tag{B7}$$

Substituting Eq. (B5) into Eq. (B7), we find the bound

$$\left|\frac{\partial}{\partial \nu_B} A^{\pi^0 N \to \eta N}\Big|_0\right| \leq \frac{2}{\pi}\int_{x_0}^{\infty}\frac{dx'}{(x')^2}\frac{4\pi(W'+M_N)}{[(p'_{10}+M_N)(p'_{20}+M_N)]^{1/2}}\left|\mathrm{Im} f_{0+}^{\pi^0 N\to\eta N}(x')\right| + \frac{2}{\pi}\int_{x_0}^{\infty}\frac{dx'}{(x')^2}\frac{4\pi(W'-M_N)}{[(p'_{10}-M_N)(p'_{20}-M_N)]^{1/2}}\left|\mathrm{Im} f_{1-}^{\pi^0 N\to\eta N}(x')\right|. \tag{B8}$$

To proceed further, we use resonance dominance to approximate the inelastic amplitude imaginary parts appearing in Eq. (B8) by

$$\mathrm{Im} f_{0+}^{\pi^0 N\to\eta N}(x') \approx \frac{g_{0+}^{\eta}}{g_{0+}^{\pi^0}}\mathrm{Im} f_{0+}^{\pi^0 N\to\pi^0 N}(x'), \quad \mathrm{Im} f_{1-}^{\pi^0 N\to\eta N}(x') \approx \frac{g_{1-}^{\eta}}{g_{1-}^{\pi^0}}\mathrm{Im} f_{1-}^{\pi^0 N\to\pi^0 N}(x'), \tag{B9}$$

with g^{η,π^0} the η,π^0 couplings to the resonance in question. Using the optical theorem to evaluate the right-hand side of Eq. (B9),

$$\mathrm{Im} f^{\pi^0 N\to\pi^0 N} = \frac{|q_\pi|}{4\pi}\sigma_{\pi^0 N}, \tag{B10}$$

combining Eqs. (B8)–(B10) in the narrow-resonance approximation, and expressing the coupling ratios g^{η}/g^{π} in terms of resonance partial widths Γ_{η,π^0} and q values $q_{\eta,\pi}$, yields the final formula

$$\left|\frac{\partial}{\partial \nu_B} A^{\pi^0 N\to\eta N}\Big|_0\right| \leq \frac{2}{\pi}\left[\frac{1}{x^2}\frac{(W+M_N)|q_\pi|}{[(p_{10}+M_N)(p_{20}+M_N)^{1/2}}\left(\frac{\Gamma_\eta}{\Gamma_{\pi^0}}\frac{|q_\pi|}{|q_\eta|}\right)^{1/2}\int\sigma_{\pi^0 N}dx\right]_{N^*(1535)} + \frac{2}{\pi}\left[\frac{1}{x^2}\frac{(W-M_N)[(p_{10}+M_N)(p_{20}+M_N)]^{1/2}}{|q_\eta|}\left(\frac{\Gamma_\eta}{\Gamma_{\pi^0}}\frac{|q_\pi|}{|q_\eta|}\right)^{1/2}\int\sigma_{\pi^0 N}dx\right]_{N^*(1470)}. \tag{B11}$$

Remembering that the branching ratio of an $I=\frac{1}{2}$ state into π^0 relative to all pionic modes is $\frac{1}{3}$, and taking $|q_\eta| \sim 182$ MeV for the nominally forbidden decay $N^*(1470) \to N\eta$ (corresponding to resonance half maximum), we find numerically that the ratio R defined in Eq. (B3) is given by

$$R \lesssim R_{N^*(1535)} + R_{N^*(1470)} = 0.014 + 0.074 \approx 0.09. \tag{B12}$$

Hence the $O(q)$ corrections appear to be substantially less important in the isoscalar octet axial-vector case than they are in the isovector axial-vector case, and so we neglect them. We similarly neglect the $O(q)$ corrections in the unitary singlet axial-vector amplitude, although an analogous argument is not possible in this case since the ninth axial current does not satisfy a PCAC equation.[24] We caution[47] in closing that the above argument is very crude at best, particularly since the $N^*(1470)$ contribution to Eq. (B11) depends as $|q_\eta|^{-3/2}$ on the q_η value assumed for the $N^*(1470) \to N\eta$ mode.

We next estimate the extent to which the order-q corrections of Eq. (43a) are already included in the basic pion-production model as a result of unitarization of the (3,3) multipoles. Using the fact that at $k^2=0$ the electric and longitudinal (3,3) multipoles are approximately related by[6]

$$\mathcal{L}_{1+}^{(3/2)} \approx -\tfrac{1}{2}\mathcal{E}_{1+}^{(3/2)}, \tag{B13}$$

a simple calculation shows that

$$[A_1^{(-)} - A_1^{(-)B}]|_0 \approx -\frac{1}{3}\left.\frac{\mathcal{E}_{1+}^{(3/2)} - \mathcal{E}_{1+}^{(3/2)B}}{|\vec{q}|}\right|_0, \qquad [A_3^{(+)} - A_3^{(+)B}]|_0 \approx -\frac{4}{3}\left.\frac{\mathcal{E}_{1+}^{(3/2)} - \mathcal{E}_{1+}^{(3/2)B}}{|\vec{q}|}\right|_0, \tag{B14}$$

where as in the text the superscript B indicates the Born approximation. To evaluate the right-hand side of Eq. (B14), we employ the partial-wave dispersion relation satisfied by $\mathcal{E}_{1+}^{(3/2)}$, which [using Eq. (B13) and making a static nucleon expansion through terms of order M_N^{-1}] takes the simple approximate form

$$\frac{(W+M_N)\mathcal{E}_{1+}^{(3/2)}}{WO_{1+}|\vec{q}|} = \frac{(W+M_N)\mathcal{E}_{1+}^{(3/2)B}}{WO_{1+}|\vec{q}|} + \frac{1}{\pi}\int_{M_\pi}^{\infty}d\omega'\left[\frac{(W'+M_N)\,\mathrm{Im}\mathcal{E}_{1+}^{(3/2)'}}{W'O'_{1+}|\vec{q}'|}\right]\left(\frac{1}{\omega'-\omega} + \frac{11}{36M_N} + \frac{1}{9}\frac{1}{\omega'+\omega}\right), \tag{B15}$$

$$\omega = W - M_N, \quad O_{1+} = [(p_{10}+M_N)(p_{20}+M_N)]^{1/2}.$$

Hence we get

$$\left.\frac{\mathcal{E}_{1+}^{(3/2)} - \mathcal{E}_{1+}^{(3/2)B}}{|\vec{q}|}\right|_0 = \frac{1}{\pi}\int_{M_\pi}^{\infty}d\omega'\left[\frac{M_N}{W'}\frac{(W'+M_N)}{O'_{1+}}\frac{\mathrm{Im}\mathcal{E}_{1+}^{(3/2)'}}{|\vec{q}'|}\right]\left(\frac{10}{9}\frac{1}{\omega'} + \frac{11}{36M_N}\right); \tag{B16}$$

integrating the right-hand side numerically, using Eq. (40.22) of Ref. 6 for $\mathcal{E}_{1+}^{(3/2)}$, gives -0.63 in units in which $M_\pi = 1$. Finally, as a point of consistency, we note that a simple calculation shows that Eq. (B16) makes no contribution to the amplitudes $[A_2^{(-)} - A_2^{(-)B}]|_0$ and $[A_4^{(-)} - A_4^{(-)B}]|_0$ which are determined by the zeroth-order PCAC relations of Eq. (42).

APPENDIX C

We give here the nuclear charge-exchange corrections calculation needed to extract the free-nucleon target ratio of Eq. (62) from the measured value of Eqs. (60)–(61). We use the averaged recipe of Eq. (24) of Ref. 40, as extended[50] to the case of nuclei with a neutron excess. In order to simultaneously treat all of the nuclei of current experimental interest,[51] we have performed the calculation outlined in Sec. II B of Ref. 50 using a simple "uniform-well" parameterization of the nuclear density, characterized by a well radius R, a nucleon density ρ, and an rms charge radius a, given by[52]

$$\rho = \frac{A}{\frac{4}{3}\pi R^3}, \qquad R = (\tfrac{5}{3})^{1/2} a, \qquad a \approx (0.82A^{1/3} + 0.58)\ \mathrm{F}. \tag{C1}$$

For each nucleus of interest we have calculated two W-averaged charge exchange matrices, one (labeled resonant) appropoiate to the (3, 3) dominated BNL cross section for $\nu + p \to \mu^- + p + \pi^+$, the other (labeled nonresonant) appropriate to the $d\sigma/dW$ curve labeled "Isoscalar pure F_1" in Fig. 7. The results are summarized[53] in Table VIII. In the case of the $I = 0$ nucleus $_6C^{12}$, the resonant matrix of Table VIII implies averaged charge-exchange parameters $\bar{a} = 0.812$, $\bar{d} = 0.137$, $\bar{c} = 0.0392$, in satisfactory agreement with the val-

TABLE VIII. Resonant and nonresonant averaged nuclear charge-exchange matrices for low-invariant-mass ($W \leq 1.4$ GeV) weak pion production. The matrix elements are to be read according to the scheme

$$[I] = \begin{bmatrix} I_{++} & I_{+0} & I_{+-} \\ I_{0+} & I_{00} & I_{0-} \\ I_{-+} & I_{-0} & I_{--} \end{bmatrix}.$$

See Appendix C for further details.

T	$[I_T^{\mathrm{res}}]$	$[I_T^{\mathrm{nonres}}]$
$_6C^{12}$	$\begin{bmatrix} 0.669 & 0.111 & 0.0318 \\ 0.111 & 0.589 & 0.111 \\ 0.0318 & 0.111 & 0.669 \end{bmatrix}$	$\begin{bmatrix} 0.685 & 0.0866 & 0.0208 \\ 0.0866 & 0.620 & 0.0866 \\ 0.0208 & 0.0866 & 0.685 \end{bmatrix}$
$_{10}Ne^{20}$	$\begin{bmatrix} 0.606 & 0.117 & 0.0390 \\ 0.117 & 0.529 & 0.117 \\ 0.0390 & 0.117 & 0.606 \end{bmatrix}$	$\begin{bmatrix} 0.626 & 0.0914 & 0.0257 \\ 0.0914 & 0.560 & 0.0914 \\ 0.0257 & 0.0914 & 0.626 \end{bmatrix}$
$_9F^{19}$	$\begin{bmatrix} 0.607 & 0.109 & 0.0348 \\ 0.120 & 0.534 & 0.113 \\ 0.0419 & 0.124 & 0.619 \end{bmatrix}$	$\begin{bmatrix} 0.628 & 0.0854 & 0.0229 \\ 0.0940 & 0.566 & 0.0879 \\ 0.0276 & 0.0968 & 0.637 \end{bmatrix}$
$_{13}Al^{27}$	$\begin{bmatrix} 0.565 & 0.113 & 0.0398 \\ 0.121 & 0.494 & 0.116 \\ 0.0453 & 0.124 & 0.574 \end{bmatrix}$	$\begin{bmatrix} 0.588 & 0.0888 & 0.0263 \\ 0.0950 & 0.526 & 0.0908 \\ 0.0300 & 0.0971 & 0.594 \end{bmatrix}$
$_{35}Br^{80}$	$\begin{bmatrix} 0.428 & 0.0958 & 0.0397 \\ 0.119 & 0.378 & 0.106 \\ 0.0613 & 0.132 & 0.458 \end{bmatrix}$	$\begin{bmatrix} 0.459 & 0.0777 & 0.0270 \\ 0.0972 & 0.412 & 0.0846 \\ 0.0419 & 0.106 & 0.482 \end{bmatrix}$

ues $\bar{a}=0.811$, $\bar{d}=0.138$, $\bar{c}=0.0450$ given in Table VII of Ref. 40 and obtained by using a "harmonic-well" parameterization of the nuclear density. Given the matrices $[I_T]$ of Table VIII, observed pion-production cross sections are related to free-nucleon cross sections by the following recipe: Let the experimental target contain the mass fractions f_T of the nuclear species with $Z=Z_T$, $A=A_T$. Then the observed cross section per nucleon is given by

$$\begin{bmatrix}\sigma(\text{obs};\pi^+)\\ \sigma(\text{obs};\pi^0)\\ \sigma(\text{obs};\pi^-)\end{bmatrix}=\sum_T f_T[I_T]\begin{bmatrix}\sigma(N_T;\pi^+)\\ \sigma(N_T;\pi^0)\\ \sigma(N_T;\pi^-)\end{bmatrix} \tag{C2}$$

with N_T an effective free-nucleon target given by

$$N_T=\frac{Z_T}{A_T}p+\left(1-\frac{Z_T}{A_T}\right)n. \tag{C3}$$

As an illustration, we apply Eq. (C3) in the BNL case of a mainly carbon and aluminum target. Assuming charged-current pion production to be purely resonant, and neutral-current pion production to be purely nonresonant, we have

$$R_0'=\frac{\sigma(\text{obs};\pi^0\nu)}{2\sigma(\text{obs};\pi^0\mu^-)};$$

$$\sigma(\text{obs};\pi^0\nu)=\sum_{T=C,\text{Al}} f_T \sum_{j=+,0,-}[I_T^{\text{nonres}}]_{0j}\,\sigma(N_T;\pi^j\nu), \tag{C4}$$

$$\sigma(\text{obs};\pi^0\mu^-)=\sum_{T=C,\text{Al}} f_T \sum_{j=+,0,-}[I_T^{\text{res}}]_{0j}\,\sigma(N_T;\pi^j\mu^-).$$

Using the BNL target fractions $f_C=\frac{1}{4}$, $f_{\text{Al}}=\frac{3}{4}$ and assuming an isoscalar neutral current, which implies

$$\sigma(n;\pi^0\nu)=\sigma(p;\pi^0\nu)=\tfrac{1}{2}\sigma(n;\pi^-\nu)=\tfrac{1}{2}\sigma(p;\pi^+\nu), \tag{C5}$$

Eq. (C4) reduces after some simple algebra to[54]

$$2R_0\equiv\frac{\sigma(n+p;\pi^0\nu)}{\sigma(n;\pi^0\mu^-)}=2R_0'\times 0.727(1+0.22r_1+0.23r_2) \tag{C6}$$

with $r_{1,2}$ the charged-current π^+ to π^0 ratios

$$r_1=\frac{\sigma(p;\pi^+\mu^-)}{\sigma(n;\pi^0\mu^-)},\quad r_2=\frac{\sigma(n;\pi^+\mu^-)}{\sigma(n;\pi^0\mu^-)}. \tag{C7}$$

Direct measurements of $r_{1,2}$ in the BNL flux are unavailable, so we have either to use theoretical values for these ratios, or to extrapolate them from the ANL measurements, neglecting possible variations with neutrino energy. The theoretical cross sections tabulated in the fourth and fifth columns of Table III give, respectively,

$$r_1=2.91,\quad r_2=0.88\quad\text{without } O(q)\text{ corrections}, \tag{C8a}$$

$$r_1=4.01,\quad r_2=1.34\quad\text{with } O(q)\text{ corrections}, \tag{C8b}$$

while preliminary ANL data give

$$r_1=3.74\pm0.86,\quad r_2=1.14\pm0.3. \tag{C8c}$$

Substituting into Eq. (C6), Eqs. (C8a)–(C8c) give, respectively,

$$\begin{aligned}2R_0&=2R_0'\times 1.59\ \text{from (C8a)},\\ 2R_0&=2R_0'\times 1.34\ \text{from (C8b)},\\ 2R_0&=2R_0'\times 1.52\pm0.15\ \text{from (C8c)}.\end{aligned} \tag{C9}$$

A charge-exchange correction factor of 1.4 has been assumed in getting Eq. (62) of the text.

---

*Research sponsored in part by the U. S. Atomic Energy Commission under Grant No. AT(11-1)-2220.

[1]F. J. Hasert *et al.*, Phys, Lett. 46B, 138 (1973); A. Benvenuti *et al.*, Phys. Rev. Lett. 32, 800 (1974).

[2]P. A. Schreiner, Argonne National Laboratory Report No. ANL/HEP 7436 (unpublished); S. J. Barish, Bull. Am. Phys. Soc. 20, 86 (1975); D. Carmony (unpublished).

[3]Columbia-Illinois-Rockefeller collaboration, data presented at the Argonne Symposium on Neutral Currents, March 6, 1975 and the Paris Weak Interactions Symposium, March 18-20, 1975.

[4]S. L. Adler, Phys. Rev. Lett. 33, 1511 (1974). In treating the $O(q)$ additions in our original ANL data analysis, we neglected to subtract away the resonant multipole contributions, as we have done following Eq. (43a) of the text. The pion production coefficients of Table V and the discussion of Sec. IV B follow the original analysis, and hence are subject to small corrections (of order 10% in the cross-section bounds). Everywhere else in the paper we use $O(q)$ additions which have the resonant multipole contributions subtracted out, as in Eqs. (43c) and (43d).

[5]S. L. Adler, E. W. Colglazier, Jr., J. B. Healy, I. Karliner, J. Lieberman, Y. J. Ng, and H.-S. Tsao, Phys. Rev. D (to be published); S. L. Adler, R. F. Dashen, J. B. Healy, I. Karliner, J. Lieberman, Y. J. Ng, and H.-S. Tsao, *ibid.* (to be published).

[6]S. L. Adler, Ann. Phys. (N.Y.) 50, 189 (1968). [See also S. L. Adler, Phys. Rev. D 9, 229 (1974).] We have taken the axial-vector form-factor mass as $M_A=0.9$ GeV.

[7]See, for example, S. L. Adler and R. F. Dashen, *Current Algebras* (Benjamin, New York, 1968).

[8]We follow throughout the metric and γ-matrix conventions of J. D. Bjorken and S. D. Drell, *Relativistic Quantum Fields* (McGraw-Hill, New York, 1965), Appendix A. Also, throughout this paper ν will be understood to mean a muon neutrino ν_μ

[9]For a more detailed discussion, see S. L. Adler and W. I. Weisberger, Phys. Rev. 169, 1392 (1968).

[10]The equal-time commutator term also vanishes for π^0 production by an arbitrary V, A neutral current, and so Eq. (12) holds in this case as well. Vanishing of the equal-time commutator in the isoscalar V, A case was noted by J. J. Sakurai, in *Neutrinos—1974*, proceedings of the Fourth International Conference on Neutrino Physics and Astrophysics, Philadelphia, 1974, edited by C. Baltay (A.I.P., New York, 1974).

[11]The Argonne flux is given, for example, in P. A. Schreiner and F. von Hippel, Argonne National Laboratory Report No. ANL/HEP 7309 (unpublished).

[12]See P. A. Schreiner, Ref. 2.

[13]We make this assumption throughout our discussion of bounds on ANL threshold pion production.

[14]In our discussion of the BNL data in Sec. IV C, the effect of cuts used in setting the relevant CERN bound on $\sigma(\nu+p\to\nu+p)$ will be explicitly taken into account.

[15]B. C. Barish *et al.*, Phys. Rev. Lett. 34, 538 (1975).

[16]We follow here the notation of S. L. Adler, E. W. Colglazier, Jr., J. B. Healy, I. Karliner, J. Lieberman, Y. J. Ng, and H.-S. Tsao, Phys. Rev. D 11, 3309 (1975).

[17]J. D. Bjorken, Phys. Rev. 179, 1547 (1969).

[18]We follow closely a treatment given in unpublished lecture notes of C. G. Callan.

[19]E. A. Paschos and L. Wolfenstein, Phys. Rev. D 7, 91 (1973).

[20]These equations, in the Weinberg-Salam-model context, were first obtained by A. Pais and S. B. Treiman, Phys. Rev. D 6, 2700 (1972).

[21]A succinct review is given in O. Nachtmann, Nucl. Phys. B38, 397 (1972).

[22]See, for example, L. M. Sehgal, Nucl. Phys. B65, 141 (1973).

[23]In equation (38a) we use the fact that for the axial-vector octet, $\alpha=D/(D+F)\approx 0.66$.

[24]In the quark model, one finds $g_A^{(0)}(0)=g_A^{(8)}(0)\approx 0.74$ and $2M_N F_2^{(0)}(0)/F_1^{(0)}(0)=2M_N F_2^{(8)}(0)/F_1^{(8)}(0)\approx -0.1$. The prediction for $F_2^{(8)}(0)$ is in excellent agreement with experiment [cf. Eq. (38b)], and so it is likely that the quark-model prediction for $F_2^{(0)}(0)$ will also be reliable. Although the quark-model prediction for $g_A^{(8)}(0)$ is in satisfactory accord with experiment [cf. Eq. (38a)] the prediction for $g_A^{(0)}(0)$ may prove unreliable because of the apparently peculiar properties (such as a possible divergence anomaly) of the ninth axial-vector current. For a discussion of issues connected with the ninth axial-current anomaly and further references, see W. A. Bardeen, Nucl. Phys. B75, 246 (1974).

[25]S. L. Adler, Phys. Rev. 137, B1022 (1965); 139, B1638 (1965).

[26]G. F. Chew, M. L. Goldberger, F. E. Low, and Y. Nambu, Phys. Rev. 106, 1345 (1957).

[27]In writing Eqs. (42) and (43) we have followed the notations of Ref. 6, which differ from those of the present paper. Thus, the superscript (0) was used in Ref. 6 to denote matrix elements of the isoscalar electromagnetic current, which would be proportional to amplitudes denoted by (8) in our present notation. Similarly, spacelike k^2 is positive in the notation of Ref. 6, but negative in our present notation. In writing Eqs. (42) we have replaced the off-shell pion-nucleon coupling $g_\gamma(0)$ by the on-shell coupling g_γ. In the numerical evaluation of Eq. (43a) we have used $\mu^V\approx 3.70$ and have taken the values of the pion nucleon amplitudes $\bar{B}^{\pi\mathcal{N}(-)}$, $(\partial/\partial\nu_B)\bar{A}^{\pi\mathcal{N}(+)}$ at the crossing-symmetric point from the tabulation of H. Pilkuhn *et al.*, Nucl. Phys. B65, 460 (1973). The theoretical analysis leading to Eqs. (42) and (43a) is described in detail in Sec. V of Ref. 6. [See particularly Eqs. (5A.21), (5A.22), (5A.9), and (5A.30).]

[28]F. E. Low, Phys. Rev. 110, 974 (1958); S. L. Adler and Y. Dothan, *ibid.* 151, 1267 (1966).

[29]The axial-vector form-factor dipole mass is ≈ 0.90 GeV, while the dipole mass appearing in the vector-current Sachs form factors is 0.84 GeV.

[30]The experimental points are taken from Fig. 10 of B. Musgrave, Argonne National Laboratory Report No. ANL/HEP 7453 (unpublished).

[31]The ANL result for M_A is $M_A=(0.90\pm 0.10)$ GeV, and we have used the central value of 0.90 GeV in all of the numerical work. Increasing M_A above the central value will bring the theoretical curves in Fig. 1 closer to the experimental points. For example, an M_A of 1.00 GeV gives cross sections 6–9% larger than those in the figure.

[32]The experimental values were obtained from B. Musgrave, private communication.

[33]The histogram was taken from Fig. 2 of P. A. Schreiner and F. von Hippel, Ref. 11.

[34]The histograms were taken from Fig. 16 of B. Musgrave, Ref. 30.

[35]The induced pseudoscalar from factor h_A makes a vanishing contribution to neutral-current reactions.

[36]This has been checked in one case, by comparing formulas obtained from the λ_4, λ_5 terms of Eq. (44) with the corresponding formulas which are obtained when the nucleon isoscalar electromagnetic form factors $F_{1,2}^S(k^2)$ are used in the final two terms of Eq. (44).

[37]S. Weinberg, Phys. Rev. Lett. 19, 1264 (1967); 27, 1688 (1972); A. Salam, in *Elementary Particle Theory: Relativistic Groups and Analyticity* (Nobel Symposium No. 8), edited by N. Svartholm (Almqvist and Wiksell, Stockholm, 1968), p. 367.

[38]The BNL flux table has been furnished to me by W. Y. Lee and L. Litt (private communication).

[39]The error ± 0.06 largely represents systematic uncertainties; the statistical error is considerably smaller (W. Y. Lee, private communication).

[40]S. L. Adler, S. Nussinov, and E. A. Paschos, Phys. Rev. D 9, 2125 (1974).

[41]For example, in the static limit the cross section for (3,3) excitation by $\mathfrak{F}_3^{5\lambda}$ is $0.202/0.263=0.77$ times that for (3,3) excitation by $\mathfrak{F}_3^{\lambda}$; see S. L. Adler, Ref. 6; B. W. Lee, Phys. Lett. 40B, 420 (1972).

[42]The uncut elastic cross-section coefficients are not used in the maximization calculation, but are included for completeness. When no cuts are made, $\sigma^{\rm BNL}(\nu+n\to\mu^-+p)=0.88\times 10^{-38}$ cm^2.

[43]D. C. Cundy *et al.*, Phys. Lett. 31B, 478 (1970). The CERN neutrino flux is given in D. H. Perkins, in *Pro-*

ceedings of the Fifth Hawaii Topical Conference in Particle Physics, 1973, edited by P. N. Dobson, Jr., V. Z. Peterson, and S. F. Tuan (Univ. of Hawaii Press, Honolulu, 1974), Fig. 1.6. Note that the absolute magnitude of the flux is irrelevant in flux averaging—only the shape of the spectrum matters.

[44]A preliminary account of this discussion has been given in S. L. Adler, in a talk given at the 1975 Coral Gables Conference, "Orbis Scientia II," 1975 (unpublished), and IAS report. As a result of a programming error, the curves given in Fig. 1 of the Coral Gables talk are too high; the corrected curves appear as Fig. 4 of the present paper.

[45]The curve shown for the pure F_1 case is very similar to the curve obtained for S, P, T coupling mixtures. See Ref. 5 for further details.

[46]Here we are indicating octet isoscalar amplitudes by the superscript (η); note that in Ref. 6 they were denoted by the superscript (0), while in the text of this paper they are denoted by the superscript (8), with (0) used to indicate singlet isoscalar quantities.

[47]Our notation follows that of Sec. III of Ref. 6, with $x=(W^2-M_N^2)/(2M_N)$. Note that writing an unsubtracted dispersion relation is not formally justified by a Regge analysis of $A^{\pi^0 N\to\eta N}$, since the leading Regge trajectory, the A_1 trajectory, has too high an intercept for the integral in Eq. (B4) to converge. However, a similar use of subtracted dispersion relations coupled with resonance dominance arguments gives a correct estimate of the magnitude of the isovector correction of Eqs. (43) and (B1), even though in this case also, the unsubtracted dispersion relation is formally divergent. Hence, our method in the isoscalar case is an heuristic one, motivated by methods which work in the isovector case. I wish to thank M. L. Goldberger for a helpful discussion of the Reggeology of the $\pi^0 N\to\eta N$ amplitude.

[49]See the Appendix of S. L. Adler, Phys. Rev. 137, B1022 (1965).

[50]S. L. Adler, Phys. Rev. D 9, 2144 (1974).

[51]The CERN Gargamelle group has data in freon (CF_3Br), and a bubble-chamber run at BNL in neon has been proposed. I wish to thank P. Musset and C. Baltay for raising the question of extending the calculations of Ref. 50 to other nuclei.

[52]H. R. Collard, L. R. B. Elton, and R. Hofstadter, in *Landolt-Börnstein: Numerical Data and Functional Relationships; Nuclear Radii,* edited by K.-H. Hellwege (Springer, Berlin, 1967), New Series, Group I, Vol. 2.

[53]B. R. Holstein and M. M. Sternheim are currently studying pion production in nuclei induced by incident protons, using the multiple scattering model of Ref. 50 and variants on the model which take nucleon recoil into account in a detailed way. This study should lead to an improved value of the pion absorption cross section $\sigma_{\rm abs}$, which when available will be used to recompute the charge-exchange matrices of Table VIII. In calculating Table VIII we have in the interim used the absorption cross section given in Eq. (27) of Ref. 40.

[54]Under our assumption of an isoscalar neutral current, the simple recipe of Eq. (24) of Ref. (40) gives the formula

$$2R = 2R_0' \times (1-2\tilde{d})\{1+[\tilde{d}/(1-2\tilde{d})](r_1+r_2)\}.$$

Taking the effective $\tilde{d}$ for the BNL target as $\frac{3}{4}d_{\rm AL}+\frac{1}{4}d_C\approx 0.16$, this formula gives

$$2R = 2R_0' \times 0.68[1+0.24(r_1+r_2)],$$

a result very similar to Eq. (C6).